Chapter 8
Shallow Shells

Shallow shells are open shells that have small curvatures (i.e. large radii of curvatures compared with other shell parameters such as length and width). Vlasov (1951) and Leissa (1973) describe a shallow shell as follows:

> Consider a shell outlined in part by some surface and which is a thin-walled spatial structure with a comparatively small rise above the plane covered by this structure. We call such shells shallow. If, for example, a building which has a rectangular floor plan is covered by a shell with a rise of not more than 1/5 of the smallest side of the rectangle lying in the plane of the supporting points of the structure, then we class such a spatial structure in the category of shallow shells.

These shells are sometimes referred to as curved plates. The general shell theory given in Chap. 1 can be readily applied to shallow shells. However, the general shell equations are rare complicated because the bending of a general shell is coupling with its stretching. When a shell is shallow as previous described, certain additional assumptions can be made to reduce the complexity in general shell equations considerably. The resulting set of equations is referred to as shallow shell theory. The development of the shallow shell theory is principally credited to, Leissa (1973), Leissa et al. (1984) and Qatu (2004), etc. The classical shallow shell theories (CSST) and shear deformation shallow shell theory (SDSST) are obtained by making following additional assumptions to the general shell theories (Qatu 2004):

1. The radii of curvature are very large compared to the inplane displacements (i.e., the curvature changes caused by the tangential displacement components u and v are small in a shallow shell, in comparison with changes caused by the normal component w). Also, the transverse shear forces are much smaller than the term $R_i \partial N_i / \partial i$:

$$\frac{u_i}{R_i} \ll 1 \quad \frac{Q_i}{R_i} \ll \frac{\partial N_i}{\partial i} \tag{8.1}$$

   where u_i is either of the inplane displacement components u and v; Q_i is either of the shear forces Q_α and Q_β; N_i is N_α, N_β or $N_{\alpha\beta}$; and R_i is R_α, R_β or $R_{\alpha\beta}$; The term ∂i indicates derivative with respect to either α or β;

G. Jin et al., *Structural Vibration*, DOI 10.1007/978-3-662-46364-2_8

2. The deepness term $(1 + z/R_i)$ is close to 1; where R_i can be R_α, R_β or $R_{\alpha\beta}$;
3. The shell is shallow enough to be represented by the plane coordinate systems. For the case of rectangular orthotropy, this leads to constant Lamé parameters.

It should be stressed that the shallow shell theories should be used for maximum span to minimum radius ratio of 1/2 or less.

With the progress of composite materials, shallow shells constructed by composite laminas are extensively used in many fields of modern engineering practices requiring high strength-weight and stiffness-weight ratios such as aircraft structures, space vehicles. A complete understanding of the bucking, bending, vibration and other characteristics of these shells is of particular importance. Laminated shallow shells can be formed as rectangular, triangular, trapezoidal, circular or any other planforms and various types of curvatures such as singly-curved (e.g., cylindrical), double-curved (e.g., spherical, hyperbolic paraboloidal) or other complex shapes such as turbomachinery blades. In the context of this chapter, we consider laminated shallow shells formed in rectangular planform with rectangular orthotropy, in which the fibers in each layer to the planform being straight.

In recent decades, a huge amount of research efforts have been devoted to the vibration analysis of laminated shallow shells. So far, some of the static and dynamic behaviors of these shells with classical boundary conditions had being presented precisely. Some research papers and articles oriented to such contributions may be found in following enumeration. Fazzolari and Carrera (2013) developed a hierarchical trigonometric Ritz formulation for free vibration and dynamic response analysis of doubly-curved anisotropic laminated shallow and deep shells. Reddy and Asce (1984) presented the exact solutions of the equations and fundamental frequencies for simply supported, doubly-curved, cross-ply laminated shells. Khdeir and Reddy (1997) predicted free and force vibration of cross-ply laminated composite shallow arches by a generalized modal approach. Qatu (1995a) studied natural vibration of completely free laminated composite triangular and trapezoidal shallow shells. Soldatos and Shu (1999) used the five-degrees-of-freedom shallow shell theory in the stress analysis of cross-ply laminated plates and shallow shell panels having a rectangular plan-form. Some other contributors in this subject are Dogan and Arslan (2009), Ghavanloo and Fazelzadeh (2013), Kurpa et al. (2010), Leissa and Chang (1996), Librescu et al. (1989a, b), Qatu (1995a, b, 1996, 2011), Qatu and Leissa (1991), Singh and Kumar (1996). More detailed and systematic summarizations can be seen in the excellent monographs by Leissa (1973), Qatu (2002a, b, 2004), Qatu et al. (2010), and Reddy (2003).

In this chapter, we consider vibration of thin and moderately thick laminated shallow shells with general boundary conditions. Fundamental equations of thin and thick shallow shells are presented in the first and second sections, respectively. Then, numerous vibration results of thin and thick laminated shallow shells with different boundary conditions, lamination schemes and geometry parameters are given in the third section by using the SDSST and the modified Fourier series. The results are obtained by applying the weak form solution procedure.

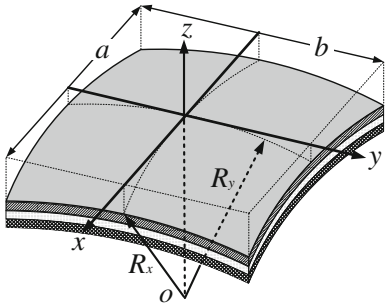

Fig. 8.1 Schematic diagram of laminated shallow shells with rectangular planform

Consider a laminated shallow shell in rectangular planform as shown in Fig. 8.1, the length, width and thickness of the shell are represented by a, b and h, respectively. The shell is shallow enough so that is can be represented by the orthogonal Cartesian coordinate system (x, y and z). The laminated shallow shell is characterized by its middle surface, which can be defined by (Qatu 2004):

$$z = -\frac{1}{2}\left(\frac{x^2}{R_x} + \frac{xy}{R_{xy}} + \frac{y^2}{R_y}\right) \tag{8.2}$$

where R_x and R_y represent the radii of curvature in the x, y directions as depicted in Fig. 8.1. R_{xy} is the corresponding radius of twist. In the present chapter, we focus on the cases when R_x, R_y and R_{xy} are constants. In addition, the x and y coordinates are conveniently oriented to be parallel to boundaries so that $R_{xy} = \infty$. The displacements of the shell in the x, y and z directions are denoted by u, v and w, respectively.

In Fig. 8.2, shallow shells constructed as various types of curvatures are plotted. It can be flat (i.e. $R_x = R_y = R_{xy} = \infty$), spherical (e.g., $R_x/R_y > 0$, $R_{xy} = \infty$), circular cylindrical (e.g., $R_y = R_{xy} = \infty$) and hyperbolic paraboloidal (e.g., $R_x/R_y < 0$, $R_{xy} = \infty$).

Considering the shallow shell in Fig. 8.1 and its Cartesian coordinate system, the coordinates, characteristics of the Lamé parameters and radius of curvatures are:

$$\alpha = x \quad \beta = y \quad A = B = 1 \quad R_\alpha = R_x \quad R_\beta = R_y \tag{8.3}$$

The equations of shallow shells are a reduction of the general shell equations given in Chap. 1 by substituting Eq. (8.3) into such shell equations.

8.1 Fundamental Equations of Thin Laminated Shallow Shells

Fundamental equations of thin laminated shallow shells are given here by substituting Eq. (8.3) into the general thin shell equations developed in Sect. 1.2. Similarly, the equations are given for the general dynamic analysis.

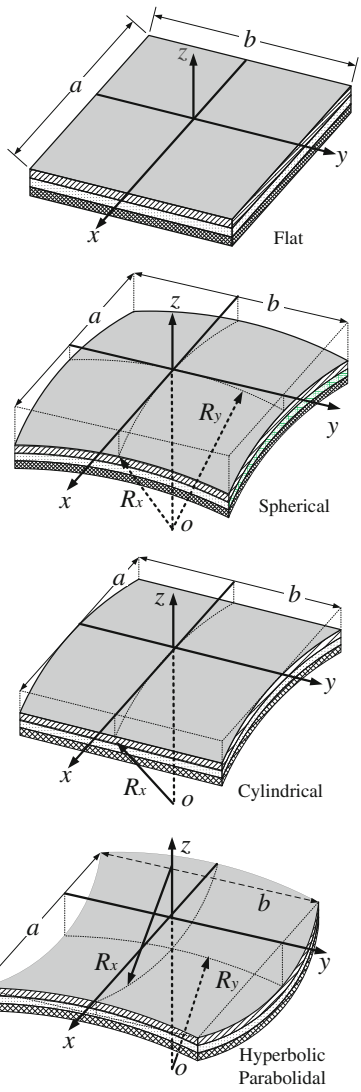

Fig. 8.2 Rectangular planform shallow shells with various types of curvatures

8.1.1 Kinematic Relations

Substituting Eq. (8.3) into Eq. (1.7), the middle surface strains and curvature changes of thin laminated shallow shells can be written in terms of middle surface displacements. Taking Eq. (8.1) into consideration, they are given as:

$$\begin{aligned}
\varepsilon_x^0 &= \frac{\partial u}{\partial x} + \frac{w}{R_x}, \quad \chi_x = -\frac{\partial^2 w}{\partial x^2} \\
\varepsilon_y^0 &= \frac{\partial v}{\partial y} + \frac{w}{R_y}, \quad \chi_y = -\frac{\partial^2 w}{\partial y^2} \\
\gamma_{xy}^0 &= \frac{\partial u}{\partial y} + \frac{\partial v}{\partial x}, \quad \chi_{xy} = -2\frac{\partial^2 w}{\partial x \partial y}
\end{aligned} \tag{8.4}$$

where ε_x^0, ε_y^0 and γ_{xy}^0 indicate the strains in middle surface; χ_x, χ_y and χ_{xy} are the curvature changes. Thus, the liner strains in the kth layer space of a laminated shallow shell can be defined as:

$$\begin{aligned}
\varepsilon_x &= \varepsilon_x^0 + z\chi_x \\
\varepsilon_y &= \varepsilon_y^0 + z\chi_y \\
\gamma_{xy} &= \gamma_{xy}^0 + z\chi_{xy}
\end{aligned} \tag{8.5}$$

where $Z_k < z < Z_{k+1}$. Z_k and Z_{k+1} denote the distances from the top surface and the bottom surface of the layer to the referenced middle surface, respectively.

8.1.2 Stress-Strain Relations and Stress Resultants

The stress-strain relations, force and moment resultants for thin laminated shallow shells formed in rectangular planform are the same as those derived earlier for thin laminated rectangular plates, see Eqs. (4.4) and (4.6).

8.1.3 Energy Functions

The strain energy (U_s) of thin laminated shallow shells during vibration can be defined in terms of middle surface strains, curvature changes and stress resultants as:

$$U_s = \frac{1}{2}\int_0^a \int_0^b \left\{ \begin{array}{l} N_x\varepsilon_x^0 + N_y\varepsilon_y^0 + N_{xy}\gamma_{xy}^0 \\ + M_x\chi_x + M_y\chi_y + M_{xy}\chi_{xy} \end{array} \right\} dxdy \tag{8.6}$$

And the kinetic energy (T) of thin laminated shallow shells during vibration is:

$$T = \frac{1}{2}\int_0^a \int_0^b I_0 \left\{ \left(\frac{\partial u}{\partial t}\right)^2 + \left(\frac{\partial v}{\partial t}\right)^2 + \left(\frac{\partial w}{\partial t}\right)^2 \right\} dxdy \tag{8.7}$$

where the inertia term I_0 is given in Eq. (1.19). Suppose q_x, q_y and q_z are the external loads in the x, y and z directions, respectively. Thus, the external work can be expressed as:

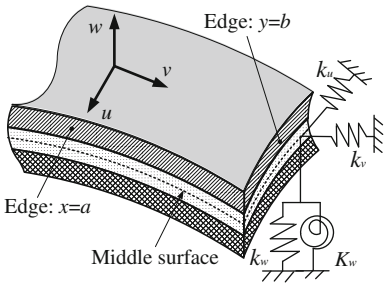

Fig. 8.3 Boundary conditions of thin laminated shallow shells

$$W_e = \int_0^a \int_0^b \{q_x u + q_y v + q_z w\} dxdy \tag{8.8}$$

The artificial spring boundary technique is adopted here to realize the general boundary conditions of a thin shallow shell. Under the current framework, symbols k_ψ^u, k_ψ^v, k_ψ^w and K_ψ^w (ψ = $x0$, $y0$, $x1$ and $y1$) are used to indicate the stiffness of the boundary spring components at the boundaries x = 0, y = 0, x = a and y = b, respectively, see Fig. 8.3. Thus, the deformation strain energy about the boundary springs (U_{sp}) can be defined as:

$$\begin{aligned} U_{sp} = & \frac{1}{2}\int_0^b \left\{ \begin{array}{l} \left[k_{x0}^u u^2 + k_{x0}^v v^2 + k_{x0}^w w^2 + K_{x0}^w(\partial w/\partial x)\right]|_{x=0} \\ + \left[k_{x1}^u u^2 + k_{x1}^v v^2 + k_{x1}^w w^2 + K_{x1}^w(\partial w/\partial x)\right]|_{x=a} \end{array} \right\} dy \\ & + \frac{1}{2}\int_0^a \left\{ \begin{array}{l} \left[k_{y0}^u u^2 + k_{y0}^v v^2 + k_{y0}^w w^2 + K_{y0}^w(\partial w/\partial y)\right]|_{y=0} \\ + \left[k_{y1}^u u^2 + k_{y1}^v v^2 + k_{y1}^w w^2 + K_{y1}^w(\partial w/\partial y)\right]|_{y=b} \end{array} \right\} dx \end{aligned} \tag{8.9}$$

8.1.4 Governing Equations and Boundary Conditions

Substituting Eq. (8.3) into Eq. (1.28) and then simplifying the expressions and taking Eq. (8.1) into consideration, the reduced governing equations of thin laminated shallow shells are:

$$\begin{array}{l} \frac{\partial N_x}{\partial x} + \frac{\partial N_{xy}}{\partial y} + q_x = I_0 \frac{\partial^2 u}{\partial t^2} \\ \frac{\partial N_{xy}}{\partial x} + \frac{\partial N_y}{\partial y} + q_y = I_0 \frac{\partial^2 v}{\partial t^2} \\ -\left(\frac{N_x}{R_x} + \frac{N_y}{R_y}\right) + \frac{\partial^2 M_x}{\partial x^2} + 2\frac{\partial^2 M_{xy}}{\partial x \partial y} + \frac{\partial^2 M_y}{\partial y^2} + q_z = I_0 \frac{\partial^2 w}{\partial t^2} \end{array} \tag{8.10}$$

Substituting Eq. (8.4) and the stress resultants equations Eq. (4.6) into Eq. (8.10), the governing equations of thin laminated shallow shells can be writing in matrix form as:

$$\left(\begin{bmatrix} L_{11} & L_{12} & L_{13} \\ L_{21} & L_{22} & L_{23} \\ L_{31} & L_{32} & L_{33} \end{bmatrix} - \omega^2 \begin{bmatrix} -I_0 & 0 & 0 \\ 0 & -I_0 & 0 \\ 0 & 0 & -I_0 \end{bmatrix} \right) \begin{bmatrix} u \\ v \\ w \end{bmatrix} = \begin{bmatrix} -p_x \\ -p_y \\ -p_z \end{bmatrix} \tag{8.11}$$

The coefficients of the linear operator L_{ij} are written as

$$\begin{aligned}
L_{11} &= \frac{\partial}{\partial x}\left(A_{11}\frac{\partial}{\partial x} + A_{16}\frac{\partial}{\partial y}\right) + \frac{\partial}{\partial y}\left(A_{16}\frac{\partial}{\partial x} + A_{66}\frac{\partial}{\partial y}\right) \\
L_{12} &= L_{21} = \frac{\partial}{\partial x}\left(A_{12}\frac{\partial}{\partial y} + A_{16}\frac{\partial}{\partial x}\right) + \frac{\partial}{\partial y}\left(A_{26}\frac{\partial}{\partial y} + A_{66}\frac{\partial}{\partial x}\right) \\
L_{13} &= \frac{\partial}{\partial x}\left(\frac{A_{11}}{R_x} + \frac{A_{12}}{R_y} - B_{11}\frac{\partial^2}{\partial x^2} - B_{12}\frac{\partial^2}{\partial y^2} - 2B_{16}\frac{\partial^2}{\partial x \partial y}\right) \\
&\quad + \frac{\partial}{\partial y}\left(\frac{A_{16}}{R_x} + \frac{A_{26}}{R_y} - B_{16}\frac{\partial^2}{\partial x^2} - B_{26}\frac{\partial^2}{\partial y^2} - 2B_{66}\frac{\partial^2}{\partial x \partial y}\right) \\
L_{22} &= \frac{\partial}{\partial x}\left(A_{26}\frac{\partial}{\partial y} + A_{66}\frac{\partial}{\partial x}\right) + \frac{\partial}{\partial y}\left(A_{22}\frac{\partial}{\partial y} + A_{26}\frac{\partial}{\partial x}\right) \\
L_{23} &= \frac{\partial}{\partial x}\left(\frac{A_{16}}{R_x} + \frac{A_{26}}{R_y} - B_{16}\frac{\partial^2}{\partial x^2} - B_{26}\frac{\partial^2}{\partial y^2} - 2B_{66}\frac{\partial^2}{\partial x \partial y}\right) \\
&\quad + \frac{\partial}{\partial y}\left(\frac{A_{12}}{R_x} + \frac{A_{22}}{R_y} - B_{12}\frac{\partial^2}{\partial x^2} - B_{22}\frac{\partial^2}{\partial y^2} - 2B_{26}\frac{\partial^2}{\partial x \partial y}\right) \\
L_{31} &= -\frac{1}{R_x}\left(A_{11}\frac{\partial}{\partial x} + A_{16}\frac{\partial}{\partial y}\right) - \frac{1}{R_y}\left(A_{12}\frac{\partial}{\partial x} + A_{26}\frac{\partial}{\partial y}\right) \\
&\quad + \frac{\partial^2}{\partial x^2}\left(B_{11}\frac{\partial}{\partial x} + B_{16}\frac{\partial}{\partial y}\right) + 2\frac{\partial^2}{\partial x \partial y}\left(B_{16}\frac{\partial}{\partial x} + B_{66}\frac{\partial}{\partial y}\right) \\
&\quad + \frac{\partial^2}{\partial y^2}\left(B_{12}\frac{\partial}{\partial x} + B_{26}\frac{\partial}{\partial y}\right) \\
L_{32} &= -\frac{1}{R_x}\left(A_{12}\frac{\partial}{\partial y} + A_{16}\frac{\partial}{\partial x}\right) - \frac{1}{R_y}\left(A_{22}\frac{\partial}{\partial y} + A_{26}\frac{\partial}{\partial x}\right) \\
&\quad + \frac{\partial^2}{\partial x^2}\left(B_{12}\frac{\partial}{\partial y} + B_{16}\frac{\partial}{\partial x}\right) + 2\frac{\partial^2}{\partial x \partial y}\left(B_{26}\frac{\partial}{\partial y} + B_{66}\frac{\partial}{\partial x}\right) \\
&\quad + \frac{\partial^2}{\partial y^2}\left(B_{22}\frac{\partial}{\partial y} + B_{26}\frac{\partial}{\partial x}\right) \\
L_{33} &= -\frac{1}{R_x}\left(\frac{A_{11}}{R_x} + \frac{A_{12}}{R_y} - B_{11}\frac{\partial^2}{\partial x^2} - B_{12}\frac{\partial^2}{\partial y^2} - 2B_{16}\frac{\partial^2}{\partial x \partial y}\right) \\
&\quad - \frac{1}{R_y}\left(\frac{A_{12}}{R_x} + \frac{A_{22}}{R_y} - B_{12}\frac{\partial^2}{\partial x^2} - B_{22}\frac{\partial^2}{\partial y^2} - 2B_{26}\frac{\partial^2}{\partial x \partial y}\right) \\
&\quad + \frac{\partial^2}{\partial x^2}\left(\frac{B_{11}}{R_x} + \frac{B_{12}}{R_y} - D_{11}\frac{\partial^2}{\partial x^2} - D_{12}\frac{\partial^2}{\partial y^2} - 2D_{16}\frac{\partial^2}{\partial x \partial y}\right) \\
&\quad + 2\frac{\partial^2}{\partial x \partial y}\left(\frac{B_{16}}{R_x} + \frac{B_{26}}{R_y} - D_{16}\frac{\partial^2}{\partial x^2} - D_{26}\frac{\partial^2}{\partial y^2} - 2D_{66}\frac{\partial^2}{\partial x \partial y}\right) \\
&\quad + \frac{\partial^2}{\partial y^2}\left(\frac{B_{12}}{R_x} + \frac{B_{22}}{R_y} - D_{12}\frac{\partial^2}{\partial x^2} - D_{22}\frac{\partial^2}{\partial y^2} - 2D_{26}\frac{\partial^2}{\partial x \partial y}\right)
\end{aligned} \tag{8.12}$$

And according to Eqs. (1.29) and (1.30), the boundary conditions of thin shallow shells are:

$$
\begin{aligned}
x=0:&\begin{cases} N_x+\frac{M_x}{R_x}-k_{x0}^{u}u=0\\ N_{xy}+\frac{M_{xy}}{R_y}-k_{x0}^{v}v=0\\ Q_x+\frac{\partial M_{xy}}{\partial y}-k_{x0}^{w}w=0\\ -M_x-K_{x0}^{w}\frac{\partial w}{\partial x}=0 \end{cases}
\quad x=a:\begin{cases} N_x+\frac{M_x}{R_x}+k_{x1}^{u}u=0\\ N_{xy}+\frac{M_{xy}}{R_y}+k_{x1}^{v}v=0\\ Q_x+\frac{\partial M_{xy}}{\partial y}+k_{x1}^{w}w=0\\ -M_x+K_{x1}^{w}\frac{\partial w}{\partial x}=0 \end{cases}\\
y=0:&\begin{cases} N_{xy}+\frac{M_{xy}}{R_x}-k_{y0}^{u}u=0\\ N_y+\frac{M_y}{R_y}-k_{y0}^{v}v=0\\ Q_y+\frac{\partial M_{xy}}{\partial x}-k_{y0}^{w}w=0\\ -M_y-K_{y0}^{w}\frac{\partial w}{\partial y}=0 \end{cases}
\quad y=0:\begin{cases} N_{xy}+\frac{M_{xy}}{R_x}+k_{y1}^{u}u=0\\ N_y+\frac{M_y}{R_y}+k_{y1}^{v}v=0\\ Q_y+\frac{\partial M_{xy}}{\partial x}+k_{y1}^{w}w=0\\ -M_y+K_{y1}^{w}\frac{\partial w}{\partial y}=0 \end{cases}
\end{aligned}
\tag{8.13}
$$

In each boundary of thin laminated shallow shells, there exists 12 possible classical boundary conditions. Taking boundaries x = constant for example, the possible classical boundary conditions are given in Table 8.1, similar boundary conditions can be obtained for boundaries y = constant.

Table 8.1 Possible classical boundary conditions for thin shallow shells at each boundary of x = constant

Boundary type	Conditions
Free boundary conditions	
F	$N_x+\frac{M_x}{R_x}=N_{xy}+\frac{M_{xy}}{R_y}=Q_x+\frac{\partial M_{xy}}{\partial y}=M_x=0$
F2	$u=N_{xy}+\frac{M_{xy}}{R_y}=Q_x+\frac{\partial M_{xy}}{\partial y}=M_x=0$
F3	$N_x+\frac{M_x}{R_x}=v=Q_x+\frac{\partial M_{xy}}{\partial y}=M_x=0$
F4	$u=v=Q_x+\frac{\partial M_{xy}}{\partial y}=M_x=0$
Simply supported boundary conditions	
S	$u=v=w=M_x=0$
SD	$N_x+\frac{M_x}{R_x}=v=w=M_x=0$
S3	$u=N_{xy}+\frac{M_{xy}}{R_y}=w=M_x=0$
S4	$N_x+\frac{M_x}{R_x}=N_{xy}+\frac{M_{xy}}{R_y}=w=M_x=0$
Clamped boundary conditions	
C	$u=v=w=\frac{\partial w}{\partial x}=0$
C2	$N_x+\frac{M_x}{R_x}=v=w=\frac{\partial w}{\partial x}=0$
C3	$u=N_{xy}+\frac{M_{xy}}{R_y}=w=\frac{\partial w}{\partial x}=0$
C4	$N_x+\frac{M_x}{R_x}=N_{xy}+\frac{M_{xy}}{R_y}=w=\frac{\partial w}{\partial x}=0$

8.2 Fundamental Equations of Thick Laminated Shallow Shells

Like general thin shell theory, the classical shallow shell theory (CSST) is applicable where the thickness is smaller than 1/20 of the smallest of the wave length and/or radii of curvature (Qatu 2004). For thick shallow shells, the Kirchhoff hypothesis should be relaxed and the shear deformation and rotary inertia should be included in the formulation. Fundamental equations of thick laminated shallow shells will be derived in this section. The following equations are derived from the general shear deformation shell theory (SDST) described in Sect. 1.3 by imposing Eq. (8.3) into those of general shells.

8.2.1 Kinematic Relations

As was done for general shells and plates, we assume that normals to the undeformed middle surface remain straight but do not normal to the deformed middle surface and the shell inplane displacements are expanded in terms of shell thickness of first order expansion. Thus, the displacement field of a thick shallow shell can be expressed as

$$\begin{aligned} U(x,y,z) &= u(x,y) + z\phi_x \\ V(x,y,z) &= v(x,y) + z\phi_y \\ W(x,y,z) &= w(x,y) \end{aligned} \tag{8.14}$$

where u, v and w are the middle surface displacements of the shallow shell in the x, y and z directions, respectively, and ϕ_x and ϕ_y represent the rotations of transverse normal respect to y- and x-axes. Substituting $\alpha = x$, $\beta = y$ into Eq. (1.33) and deleting the z/R_α and z/R_β terms, the normal and shear strains at any point in the shallow shell then can be written in terms of middle surface strains and curvature changes as:

$$\begin{aligned} \varepsilon_x &= \varepsilon_x^0 + z\chi_x, \quad \gamma_{xz} = \gamma_{xz}^0 \\ \varepsilon_y &= \varepsilon_y^0 + z\chi_y, \quad \gamma_{yz} = \gamma_{yz}^0 \\ \gamma_{xy} &= \gamma_{xy}^0 + z\chi_{xy} \end{aligned} \tag{8.15}$$

Substituting Eq. (8.3) into Eq. (1.34) and taking Eq. (8.1) into consideration, the middle surface strains and curvature changes are:

$$\begin{aligned}
\varepsilon_x^0 &= \frac{\partial u}{\partial x} + \frac{w}{R_x}, \quad & \chi_x &= \frac{\partial \phi_x}{\partial x} \\
\varepsilon_y^0 &= \frac{\partial v}{\partial y} + \frac{w}{R_y}, \quad & \chi_y &= \frac{\partial \phi_y}{\partial y} \\
\gamma_{xy}^0 &= \frac{\partial v}{\partial x} + \frac{\partial u}{\partial y}, \quad & \chi_{xy} &= \frac{\partial \phi_y}{\partial x} + \frac{\partial \phi_x}{\partial y} \\
\gamma_{xz}^0 &= \frac{\partial w}{\partial x} + \phi_x, \quad & \gamma_{yz}^0 &= \frac{\partial w}{\partial y} + \phi_y
\end{aligned} \tag{8.16}$$

The above equations constitute the fundamental strain-displacement relations of a thick shallow shell formed in rectangular planform.

8.2.2 Stress-Strain Relations and Stress Resultants

The stress-strain relations and stress resultants for thick laminated shallow shells formed in rectangular planform are the same as those derived earlier for thick laminated rectangular plates, see Eqs. (4.19), (4.21) and (4.22).

8.2.3 Energy Functions

The strain energy (U_s) of thick shallow shells during vibration can be defined as

$$U_s = \frac{1}{2}\int_0^a \int_0^b \left\{ \begin{array}{l} N_x\varepsilon_x^0 + N_y\varepsilon_y^0 + N_{xy}\varepsilon_{xy}^0 + N_{yx}\varepsilon_{yx}^0 + M_x\chi_x \\ + M_y\chi_y + M_{xy}\chi_{xy} + M_{yx}\chi_{yx} + Q_y\gamma_{yz} + Q_x\gamma_{xz} \end{array} \right\} dydx \tag{8.17}$$

And the corresponding kinetic energy function (T) is:

$$T = \frac{1}{2}\int_0^a \int_0^b \left\{ \begin{array}{l} I_0\left(\frac{\partial u}{\partial t}\right)^2 + 2I_1\frac{\partial u}{\partial t}\frac{\partial \phi_x}{\partial t} + I_2\left(\frac{\partial \phi_x}{\partial t}\right)^2 + I_0\left(\frac{\partial v}{\partial t}\right)^2 \\ + 2I_1\frac{\partial v}{\partial t}\frac{\partial \phi_y}{\partial t} + I_2\left(\frac{\partial \phi_y}{\partial t}\right)^2 + I_0\left(\frac{\partial w}{\partial t}\right)^2 \end{array} \right\} dydx \tag{8.18}$$

The inertia terms I_i (i = 0, 1, 2) are written as in Eq. (1.52). Assuming the distributed external forces q_x, q_y and q_z are in the x, y and z directions, respectively and m_x and m_y represent the external couples in the middle surface, thus, the work done by the external forces and moments is

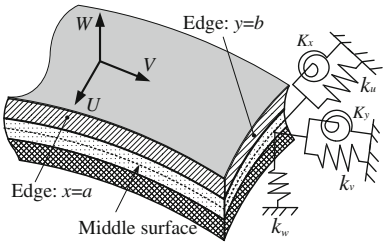

Fig. 8.4 Boundary conditions of thick laminated shallow shells

$$W_e = \int_0^a \int_0^b \{q_x u + q_y v + q_z w + m_x \phi_x + m_y \phi_y\} dy dx \tag{8.19}$$

As was done for thin laminated shallow shells, the artificial spring boundary technique is adopted here to realize the general boundary conditions of thick laminated shallow shells, in which three groups of linear springs (k_u, k_v, k_w) and two groups of rotational springs (K_x, K_y) are distributed uniformly along each shell boundary artificially, see Fig. 8.4. Therefore, the deformation strain energy (U_{sp}) of the boundary springs during vibration can be written as:

$$\begin{aligned} U_{sp} = & \frac{1}{2}\int_0^b \left\{ \begin{array}{l} \left[k_{x0}^u u^2 + k_{x0}^v v^2 + k_{x0}^w w^2 + K_{x0}^x \phi_x^2 + K_{x0}^y \phi_y^2\right]|_{x=0} \\ + \left[k_{x1}^u u^2 + k_{x1}^v v^2 + k_{x1}^w w^2 + K_{x1}^x \phi_x^2 + K_{x1}^y \phi_y^2\right]|_{x=a} \end{array} \right\} dy \\ & + \frac{1}{2}\int_0^a \left\{ \begin{array}{l} \left[k_{y0}^u u^2 + k_{y0}^v v^2 + k_{y0}^w w^2 + K_{y0}^x \phi_x^2 + K_{y0}^y \phi_y^2\right]|_{y=0} \\ + \left[k_{y1}^u u^2 + k_{y1}^v v^2 + k_{y1}^w w^2 + K_{y0}^x \phi_x^2 + K_{y0}^y \phi_y^2\right]|_{y=b} \end{array} \right\} dx \end{aligned} \tag{8.20}$$

where k_ψ^u, k_ψ^v, k_ψ^w, K_ψ^x and K_ψ^y ($\psi = x0$, $y0$, $x1$ and $y1$) represent the rigidities (per unit length) of the boundary springs at the boundaries $x = 0$, $y = 0$, $x = a$ and $y = b$, respectively. In such case, the stiffness of the boundary springs can take any value from zero to infinity to better model many real-world boundary conditions including all the classical boundaries and the uniform elastic ones. For instance, the clamped restraint condition is essentially obtained by setting the spring stiffness substantially larger than the bending rigidity of the involved shallow shell ($10^7 \times D$).

8.2.4 Governing Equations and Boundary Conditions

The governing equations and boundary conditions of thick laminated shallow shells can be derived by the Hamilton's principle in the same manner as described in

Sect. 1.2.4 or specializing from those of general thick shells. Substituting Eq. (8.3) into Eq. (1.59) and taking Eq. (8.1) into consideration, the governing equations for thick shallow shells are

$$\begin{aligned}
&\frac{\partial N_x}{\partial x}+\frac{\partial N_{xy}}{\partial y}+q_x=I_0\frac{\partial^2 u}{\partial t^2}+I_1\frac{\partial^2 \phi_x}{\partial t^2}\\
&\frac{\partial N_{xy}}{\partial x}+\frac{\partial N_y}{\partial y}+q_y=I_0\frac{\partial^2 v}{\partial t^2}+I_1\frac{\partial^2 \phi_y}{\partial t^2}\\
&-\left(\frac{N_x}{R_x}+\frac{N_y}{R_y}\right)+\frac{\partial Q_x}{\partial x}+\frac{\partial Q_y}{\partial y}+q_z=I_0\frac{\partial^2 w}{\partial t^2}\\
&\frac{\partial M_x}{\partial x}+\frac{\partial M_{xy}}{\partial y}-Q_x+m_x=I_1\frac{\partial^2 u}{\partial t^2}+I_2\frac{\partial^2 \phi_x}{\partial t^2}\\
&\frac{\partial M_{xy}}{\partial x}+\frac{\partial M_y}{\partial y}-Q_y+m_y=I_1\frac{\partial^2 v}{\partial t^2}+I_2\frac{\partial^2 \phi_y}{\partial t^2}
\end{aligned} \tag{8.21}$$

Furthermore, the above equations can be written in terms of displacements and rotation components as

$$\left(\begin{bmatrix}
L_{11} & L_{12} & L_{13} & L_{14} & L_{15}\\
L_{21} & L_{22} & L_{23} & L_{24} & L_{25}\\
L_{31} & L_{32} & L_{33} & L_{34} & L_{35}\\
L_{41} & L_{42} & L_{43} & L_{44} & L_{45}\\
L_{51} & L_{52} & L_{53} & L_{54} & L_{55}
\end{bmatrix}-\omega^2\begin{bmatrix}
M_{11} & 0 & 0 & M_{14} & 0\\
0 & M_{22} & 0 & 0 & M_{25}\\
0 & 0 & M_{33} & 0 & 0\\
M_{41} & 0 & 0 & M_{44} & 0\\
0 & M_{52} & 0 & 0 & M_{55}
\end{bmatrix}\right)\begin{bmatrix}u\\v\\w\\\phi_x\\\phi_y\end{bmatrix}=\begin{bmatrix}-p_x\\-p_y\\-p_z\\-m_x\\-m_y\end{bmatrix} \tag{8.22}$$

The coefficients of the linear operator L_{ij} are listed below

$$\begin{aligned}
L_{11}&=\frac{\partial}{\partial x}\left(A_{11}\frac{\partial}{\partial x}+A_{16}\frac{\partial}{\partial y}\right)+\frac{\partial}{\partial y}\left(A_{16}\frac{\partial}{\partial x}+A_{66}\frac{\partial}{\partial y}\right)\\
L_{12}&=\frac{\partial}{\partial x}\left(A_{12}\frac{\partial}{\partial y}+A_{16}\frac{\partial}{\partial x}\right)+\frac{\partial}{\partial y}\left(A_{26}\frac{\partial}{\partial y}+A_{66}\frac{\partial}{\partial x}\right)\\
L_{13}&=\frac{\partial}{\partial x}\left(\frac{A_{11}}{R_x}+\frac{A_{12}}{R_y}\right)+\frac{\partial}{\partial y}\left(\frac{A_{16}}{R_x}+\frac{A_{26}}{R_y}\right)\\
L_{14}&=\frac{\partial}{\partial x}\left(B_{11}\frac{\partial}{\partial x}+B_{16}\frac{\partial}{\partial y}\right)+\frac{\partial}{\partial y}\left(B_{16}\frac{\partial}{\partial x}+B_{66}\frac{\partial}{\partial y}\right)\\
L_{15}&=\frac{\partial}{\partial x}\left(B_{12}\frac{\partial}{\partial y}+B_{16}\frac{\partial}{\partial x}\right)+\frac{\partial}{\partial y}\left(B_{26}\frac{\partial}{\partial y}+B_{66}\frac{\partial}{\partial x}\right)\\
L_{21}&=\frac{\partial}{\partial x}\left(A_{16}\frac{\partial}{\partial x}+A_{66}\frac{\partial}{\partial y}\right)+\frac{\partial}{\partial y}\left(A_{12}\frac{\partial}{\partial x}+A_{26}\frac{\partial}{\partial y}\right)
\end{aligned} \tag{8.23}$$

$$
\begin{aligned}
L_{22} &= \frac{\partial}{\partial x}\left(A_{26}\frac{\partial}{\partial y}+A_{66}\frac{\partial}{\partial x}\right)+\frac{\partial}{\partial y}\left(A_{22}\frac{\partial}{\partial y}+A_{26}\frac{\partial}{\partial x}\right)\\
L_{23} &= \frac{\partial}{\partial x}\left(\frac{A_{16}}{R_x}+\frac{A_{26}}{R_y}\right)+\frac{\partial}{\partial y}\left(\frac{A_{12}}{R_x}+\frac{A_{22}}{R_y}\right)\\
L_{24} &= \frac{\partial}{\partial x}\left(B_{16}\frac{\partial}{\partial x}+B_{66}\frac{\partial}{\partial y}\right)+\frac{\partial}{\partial y}\left(B_{12}\frac{\partial}{\partial x}+B_{26}\frac{\partial}{\partial y}\right)\\
L_{25} &= \frac{\partial}{\partial x}\left(B_{26}\frac{\partial}{\partial y}+B_{66}\frac{\partial}{\partial x}\right)+\frac{\partial}{\partial y}\left(B_{22}\frac{\partial}{\partial y}+B_{26}\frac{\partial}{\partial x}\right)\\
L_{31} &= -\frac{1}{R_x}\left(A_{11}\frac{\partial}{\partial x}+A_{16}\frac{\partial}{\partial y}\right)-\frac{1}{R_y}\left(A_{12}\frac{\partial}{\partial x}+A_{26}\frac{\partial}{\partial y}\right)\\
L_{32} &= -\frac{1}{R_x}\left(A_{12}\frac{\partial}{\partial y}+A_{16}\frac{\partial}{\partial x}\right)-\frac{1}{R_y}\left(A_{22}\frac{\partial}{\partial y}+A_{26}\frac{\partial}{\partial x}\right)\\
L_{33} &= -\frac{1}{R_x}\left(\frac{A_{11}}{R_x}+\frac{A_{12}}{R_y}\right)-\frac{1}{R_y}\left(\frac{A_{11}}{R_x}+\frac{A_{12}}{R_y}\right)+\frac{\partial}{\partial x}\left(A_{45}\frac{\partial}{\partial y}+A_{55}\frac{\partial}{\partial x}\right)\\
&\quad+\frac{\partial}{\partial y}\left(A_{44}\frac{\partial}{\partial y}+A_{45}\frac{\partial}{\partial x}\right)\\
L_{34} &= -\frac{1}{R_x}\left(B_{11}\frac{\partial}{\partial x}+B_{16}\frac{\partial}{\partial y}\right)-\frac{1}{R_y}\left(B_{12}\frac{\partial}{\partial x}+B_{26}\frac{\partial}{\partial y}\right)+A_{55}\frac{\partial}{\partial x}+A_{45}\frac{\partial}{\partial y}\\
L_{35} &= -\frac{1}{R_x}\left(B_{12}\frac{\partial}{\partial y}+B_{16}\frac{\partial}{\partial x}\right)-\frac{1}{R_y}\left(B_{22}\frac{\partial}{\partial y}+B_{26}\frac{\partial}{\partial x}\right)+A_{45}\frac{\partial}{\partial x}+A_{44}\frac{\partial}{\partial y}\\
L_{41} &= \frac{\partial}{\partial x}\left(B_{11}\frac{\partial}{\partial x}+B_{16}\frac{\partial}{\partial y}\right)+\frac{\partial}{\partial y}\left(B_{16}\frac{\partial}{\partial x}+B_{66}\frac{\partial}{\partial y}\right)\\
L_{42} &= \frac{\partial}{\partial x}\left(B_{12}\frac{\partial}{\partial y}+B_{16}\frac{\partial}{\partial x}\right)+\frac{\partial}{\partial y}\left(B_{26}\frac{\partial}{\partial y}+B_{66}\frac{\partial}{\partial x}\right)\\
L_{43} &= \frac{\partial}{\partial x}\left(\frac{B_{11}}{R_x}+\frac{B_{12}}{R_y}\right)+\frac{\partial}{\partial y}\left(\frac{B_{16}}{R_x}+\frac{B_{26}}{R_y}\right)-\left(A_{45}\frac{\partial}{\partial y}+A_{55}\frac{\partial}{\partial x}\right)\\
L_{44} &= \frac{\partial}{\partial x}\left(D_{11}\frac{\partial}{\partial x}+D_{16}\frac{\partial}{\partial y}\right)+\frac{\partial}{\partial y}\left(D_{16}\frac{\partial}{\partial x}+D_{66}\frac{\partial}{\partial y}\right)-A_{55}\\
L_{45} &= \frac{\partial}{\partial x}\left(D_{12}\frac{\partial}{\partial y}+D_{16}\frac{\partial}{\partial x}\right)+\frac{\partial}{\partial y}\left(D_{26}\frac{\partial}{\partial y}+D_{66}\frac{\partial}{\partial x}\right)-A_{45}\\
L_{51} &= \frac{\partial}{\partial x}\left(B_{16}\frac{\partial}{\partial x}+B_{66}\frac{\partial}{\partial y}\right)+\frac{\partial}{\partial y}\left(B_{12}\frac{\partial}{\partial x}+B_{26}\frac{\partial}{\partial y}\right)\\
L_{52} &= \frac{\partial}{\partial x}\left(B_{26}\frac{\partial}{\partial y}+B_{66}\frac{\partial}{\partial x}\right)+\frac{\partial}{\partial y}\left(B_{22}\frac{\partial}{\partial y}+B_{26}\frac{\partial}{\partial x}\right)\\
L_{53} &= \frac{\partial}{\partial x}\left(\frac{B_{16}}{R_x}+\frac{B_{26}}{R_y}\right)+\frac{\partial}{\partial y}\left(\frac{B_{12}}{R_x}+\frac{B_{22}}{R_y}\right)-\left(A_{44}\frac{\partial}{\partial y}+A_{45}\frac{\partial}{\partial x}\right)
\end{aligned}
$$

$$
\begin{aligned}
L_{54} &= \frac{\partial}{\partial x}\left(D_{16}\frac{\partial}{\partial x}+D_{66}\frac{\partial}{\partial y}\right)+\frac{\partial}{\partial y}\left(D_{12}\frac{\partial}{\partial x}+D_{26}\frac{\partial}{\partial y}\right)-A_{45}\\
L_{55} &= \frac{\partial}{\partial x}\left(D_{26}\frac{\partial}{\partial y}+D_{66}\frac{\partial}{\partial x}\right)+\frac{\partial}{\partial y}\left(D_{22}\frac{\partial}{\partial y}+D_{26}\frac{\partial}{\partial x}\right)-A_{44}\\
M_{11} &= M_{22}=M_{33}=-I_0\\
M_{14} &= M_{41}=M_{15}=M_{51}=-I_1\\
M_{44} &= M_{55}=-I_2
\end{aligned}
$$

And according to Eqs. (1.60), (1.61) and (8.3), the general boundary conditions of thick shallow shells are

$$
\begin{aligned}
x=0:&\begin{cases}N_x-k_{x0}^{u}u=0\\ N_{xy}-k_{x0}^{v}v=0\\ Q_x-k_{x0}^{w}w=0\\ M_x-K_{x0}^{x}\phi_x=0\\ M_{xy}-K_{x0}^{y}\phi_y=0\end{cases}
\qquad
x=a:\begin{cases}N_x+k_{x1}^{u}u=0\\ N_{xy}+k_{x1}^{v}v=0\\ Q_x+k_{x1}^{w}w=0\\ M_x+K_{x1}^{x}\phi_x=0\\ M_{xy}+K_{x1}^{y}\phi_y=0\end{cases}\\
y=0:&\begin{cases}N_{yx}-k_{y0}^{u}u=0\\ N_y-k_{y0}^{v}v=0\\ Q_y-k_{y0}^{w}w=0\\ M_{yx}-K_{y0}^{x}\phi_x=0\\ M_y-K_{y0}^{y}\phi_y=0\end{cases}
\qquad
y=0:\begin{cases}N_{yx}+k_{y1}^{u}u=0\\ N_y+k_{y1}^{v}v=0\\ Q_y+k_{y1}^{w}w=0\\ M_{yx}+K_{y1}^{x}\phi_x=0\\ M_y+K_{y1}^{y}\phi_y=0\end{cases}
\end{aligned}
\tag{8.24}
$$

For thick shallow shells, there exists 24 possible classical boundary conditions in each boundary. The classification of the classical boundary conditions shown in Table 4.2 for thick rectangular plates is applicable for thick shallow shells in rectangular planform.

The classical boundary conditions of laminated shallow shells can be readily realized by applying the artificial spring boundary technique. In this chapter, we mainly consider the F, SD, S and C boundary conditions. Taking edge $x = 0$ for example, the corresponding spring rigidities for the four classical boundary conditions are given as in Eq. (4.30).

8.3 Vibration of Laminated Shallow Shells

Free vibration of laminated shallow shells formed on rectangular planforms with general boundary conditions, arbitrary lamination schemes and various types of curvatures will be considered, including shallow cylindrical, spherical and hyperbolic paraboloidal shells, see Fig. 8.2. Solutions in the framework of shear deformation shallow shell theory (SDSST) will be presented.

From Eq. (8.23), it is obvious that each displacements/rotation component of thick laminated shallow shells is required to have up to the second derivatives. Therefore, regardless of boundary conditions, each displacements/rotation component of a laminated shallow shell is expressed as the proposed modified Fourier series expansion in which several auxiliary functions are introduced to ensure and accelerate the convergence of the series expansion:

$$\begin{aligned}
u(x,y) &= \sum_{m=0}^{M}\sum_{n=0}^{N} A_{mn}\cos\lambda_m x\cos\lambda_n y + \sum_{l=1}^{2}\sum_{n=0}^{N} a_{ln}P_l(x)\cos\lambda_n y \\
&\quad + \sum_{l=1}^{2}\sum_{m=0}^{M} b_{lm}P_l(y)\cos\lambda_m x \\
v(x,y) &= \sum_{m=0}^{M}\sum_{n=0}^{N} B_{mn}\cos\lambda_m x\cos\lambda_n y + \sum_{l=1}^{2}\sum_{n=0}^{N} c_{ln}P_l(x)\cos\lambda_n y \\
&\quad + \sum_{l=1}^{2}\sum_{m=0}^{M} d_{lm}P_l(y)\cos\lambda_m x \\
w(x,y) &= \sum_{m=0}^{M}\sum_{n=0}^{N} C_{mn}\cos\lambda_m x\cos\lambda_n y + \sum_{l=1}^{2}\sum_{n=0}^{N} e_{ln}P_l(x)\cos\lambda_n y \\
&\quad + \sum_{l=1}^{2}\sum_{m=0}^{M} f_{lm}P_l(y)\cos\lambda_m x \\
\phi_x(x,y) &= \sum_{m=0}^{M}\sum_{n=0}^{N} D_{mn}\cos\lambda_m x\cos\lambda_n y + \sum_{l=1}^{2}\sum_{n=0}^{N} g_{ln}P_l(x)\cos\lambda_n y \\
&\quad + \sum_{l=1}^{2}\sum_{m=0}^{M} h_{lm}P_l(y)\cos\lambda_m x \\
\phi_y(x,y) &= \sum_{m=0}^{M}\sum_{n=0}^{N} E_{mn}\cos\lambda_m x\cos\lambda_n y + \sum_{l=1}^{2}\sum_{n=0}^{N} i_{ln}P_l(x)\cos\lambda_n y \\
&\quad + \sum_{l=1}^{2}\sum_{m=0}^{M} j_{lm}P_l(y)\cos\lambda_m x
\end{aligned} \tag{8.25}$$

where $\lambda_m = m\pi/a$ and $\lambda_n = n\pi/b$. The auxiliary functions $P_l(x)$ and $P_l(y)$ are given in Eqs. (4.32) and (4.33).

Like rectangular plates, each shallow shell formed on rectangular planforms has four boundaries. Thus, for the sake of simplicity, a four-letter string is employed to represent the boundary condition of a shallow shell, such as FCSSD identifies the shell having F, C, S and SD boundary conditions at boundaries $x = 0$, $y = 0$, $x = a$, $y = b$, respectively. Furthermore, for all numerical examples, unless otherwise stated, the layers of the considered laminated shallow shells are of equal thickness and made of the same composite material: $E_2 = 10$ GPa, $E_1/E_2 =$ open, $\mu_{12} = 0.25$,

$G_{12} = 0.6E_2$, $G_{13} = 0.6E_2$, $G_{23} = 0.5E_2$ and $\rho = 1{,}450$ kg/m^3. In addition, the natural frequencies of the considered shells will be expressed by the non-dimensional parameters as $\Omega = \omega a^2\sqrt{\rho/E_2h^2}$.

8.3.1 Convergence Studies and Result Verification

Table 8.2 shows the first six frequency parameters $\Omega = \omega a^2\sqrt{\rho/E_1h^2}$ for completely free, [30°/−30°/−30°/30°] laminated graphite/epoxy shallow cylindrical, spherical and hyperbolic paraboloidal shells with different truncation schemes (i.e. $M = N = 11, 12, 14, 15$), respectively, together with results presented by Qatu (2004).

Table 8.2 Convergence of frequency parameters $\Omega = \omega a^2\sqrt{\rho/E_1h^2}$ for [30°/−30°/−30°/30°] laminated graphite/epoxy shallow cylindrical, spherical and hyperbolic paraboloidal shells

R_y/R_x	B.C.	$M \times N$	Mode number				
			1	2	3	4	5
0	FFFF	11 × 11	1.912	2.975	4.889	6.697	8.226
		12 × 12	1.912	2.975	4.887	6.695	8.223
		14 × 14	1.912	2.974	4.885	6.693	8.219
		15 × 15	1.911	2.974	4.884	6.693	8.216
	CCCC	11 × 11	15.38	15.91	19.71	21.86	24.21
		12 × 12	15.38	15.91	19.70	21.85	24.20
		14 × 14	15.38	15.90	19.69	21.85	24.19
		15 × 15	15.38	15.89	19.69	21.85	24.18
1	FFFF	11 × 11	2.282	3.320	5.847	6.746	8.341
		12 × 12	2.280	3.318	5.843	6.742	8.333
		14 × 14	2.278	3.316	5.838	6.736	8.325
		15 × 15	2.277	3.315	5.836	6.734	8.324
		Qatu (2004)	2.283	3.323	5.871	6.781	8.394
	CCCC	11 × 11	28.54	31.05	37.24	37.94	39.44
		12 × 12	28.54	31.03	37.23	37.93	39.43
		14 × 14	28.53	31.01	37.21	37.91	39.43
		15 × 15	28.53	31.00	37.20	37.90	39.42
-1	FFFF	11 × 11	2.111	4.873	4.875	8.771	9.060
		12 × 12	2.110	4.870	4.874	8.767	9.055
		14 × 14	2.109	4.866	4.872	8.762	9.048
		15 × 15	2.108	4.865	4.871	8.761	9.046
		Qatu (2004)	2.115	4.882	4.887	8.809	9.106
	CCCC	11 × 11	22.05	24.51	27.85	27.87	32.86
		12 × 12	22.04	24.51	27.84	27.86	32.83
		14 × 14	22.04	24.49	27.83	27.84	32.81
		15 × 15	22.04	24.49	27.82	27.83	32.81

The FFFF and CCCC boundary conditions are performed in the study. The geometry and material constants of the layers of the considered shells are given as: $b/a = 1$, $h/a = 0.01$, $R_y/a = 2$, $E_1 = 138$ GPa, $E_2 = 8.96$ GPa $\mu_{12} = 0.3$, $G_{12} = G_{13} = 7.1$ GPa, $G_{23} = 3.9$ GPa. It is obvious that the modified Fourier series solution converges quickly. The maximum difference between the 11 × 11-term solutions and those of 15 × 15-term is less than 0.24 %. Based on this analysis, the truncated number of the displacement expressions will be uniformly selected as $M = N = 15$ in all subsequent calculations. Furthermore, by comparing with results published by Qatu (2004), we can find a well agreement between the two results. The differences between these two results are attributed a different shallow theory was used by Qatu (2004).

Table 8.3 shows the comparison of the fundamental parameters Ω for cross-ply cylindrical, spherical and hyperbolic paraboloidal shallow shells with SDSDSDSD boundary conditions and different curvature ratios (a/R). The shells are composed of graphite/epoxy ($E_1/E_2 = 15$, $\mu_{12} = 0.25$, $G_{12} = G_{13} = G_{23} = 0.5E_2$) and having geometry properties: $a/b = 1$, $h/a = 0.1$. The symmetric lamination [0°/90°/90°/0°] and two asymmetric laminations [0°/90°] and [90°/0°] are used in the comparison. "–" represents results that were not considered in the referential work. Curvature ratios are varied from 0 (flat plate) to 0.5 (limit of shallow shell theory). The table shows that the present solutions match very well with those reported by Qatu (2004). Except the case of shallow cylindrical shell with [90°/0°] and curvature ratio $a/R = 0.5$, the maximum differences between the two results are less than 1.12, 0.012 and 0.012 % for the shallow cylindrical, spherical and hyperbolic paraboloidal shells, respectively.

Table 8.4 shows the comparison of the fundamental parameters Ω for a three-layered, [0°/90°/0°] shallow spherical shell with different boundary conditions and

Table 8.3 Comparison of the fundamental frequency parameters Ω for cross-ply cylindrical, spherical and hyperbolic paraboloidal shallow shells with SDSDSDSD boundary conditions and different curvature ratios

R_y/R_x	a/R_y	SDSST (Qatu 2004)			Present		
		[0°/90°]	[90°/0°]	[0°/90°/90°/0°]	[0°/90°]	[90°/0°]	[0°/90°/90°/0°]
0	0	8.1196	8.1196	10.972	8.1205	8.1205	10.972
	0.1	8.1259	8.1448	10.987	8.1268	8.1602	10.987
	0.2	8.1774	8.1538	11.032	8.1783	8.2454	11.032
	0.5	8.5784	8.0831	11.334	8.5790	8.7529	11.335
+1	0	–	8.1196	10.972	8.1205	8.1205	10.972
	0.1	–	8.2190	11.043	8.2199	8.2199	11.043
	0.2	–	8.5084	11.252	8.5092	8.5092	11.253
	0.5	–	10.249	12.572	10.249	10.249	12.571
−1	0	8.1196	8.1196	10.972	8.1205	8.1205	10.972
	0.1	8.0785	8.1448	10.961	8.0794	8.1458	10.961
	0.2	8.0223	8.1538	10.927	8.0233	8.1548	10.928
	0.5	7.7739	8.0831	10.703	7.7748	8.0841	10.704

Table 8.4 Comparison of the fundamental frequency parameters Ω for a three-layered, [0°/90°/0°] shallow spherical shell with different boundary conditions and curvature ratios

Theory	a/R_y	Boundary conditions					
		FSFS	FSSS	FSCS	SSSS	SSCS	CSCS
Present	0	3.788	4.320	6.144	12.163	14.248	16.383
	0.05	3.795	4.325	6.146	12.179	14.265	16.487
	0.20	3.898	4.404	6.164	12.417	14.514	17.966
SDSST (Librescu et al. 1989a)	0	3.788	4.320	6.144	12.163	14.248	16.383
	0.05	3.794	4.325	6.146	12.178	14.264	16.487
	0.20	3.891	4.397	6.163	12.394	14.499	17.959
Difference (%)	0	0.01	0.01	0.01	0.00	0.00	0.00
	0.05	0.02	0.00	0.01	0.01	0.01	0.00
	0.20	0.17	0.16	0.01	0.19	0.11	0.04

curvature ratios (a/R). The shell having SD boundary conditions at the edges $y = 0$, $y = b$ and the other two edges having arbitrary boundary conditions. The shell is formed on square planform and composed of composite layers having following material and geometry parameters: $a/b = 1$, $h/a = 0.1$, $E_1/E_2 = 25$, $\mu_{12} = 0.25$, $G_{12} = G_{13} = 0.5E_2$, $G_{23} = 0.2E_2$. The state space solutions provided by Librescu et al. (1989a) are selected as the benchmark solutions. Comparing the two results, we can find that the current solutions match very well with the referential data. The maximum difference between the two results is very small and less than 0.17 %.

8.3.2 *Laminated Shallow Shells with General Boundary Conditions*

Table 8.5 shows the first four non-dimension frequency parameters Ω of a three-layered, [0°/90°/0°] shallow cylindrical shell with different boundary conditions and thickness-length ratios. Four different thickness-length ratios i.e. $h/a = 0.01$, 0.05, 0.1 and 0.15, corresponding to thin to thick shallow shells are performed in the analysis. The shell parameters used are: $a/b = 1$, $R_x = \infty$, $a/R_y = 0.1$, $E_1/E_2 = 15$. It can be seen from the table that the augmentation of the thickness-length ratio leads to the decrease of the frequency parameters. Tables 8.6 and 8.7 show the similar results for shallow spherical ($a/R_x = a/R_y = 0.1$) and hyperbolic paraboloidal ($a/R_x = 0.1$, $a/R_y = -0.1$) shells, respectively. The similar observation can be seen in the tables as well. In addition, comparing the three tables, it can be found that the frequency parameters of the hyperbolic paraboloidal shell are higher than the cylindrical and spherical ones. And the results of the shallow cylindrical shell are the smallest. Furthermore, from Table 8.5, we can see that frequency parameters of

Table 8.5 Frequency parameters Ω for a three-layered, [0°/90°/0°] shallow cylindrical shell with different boundary conditions and thickness-length ratios ($a/b = 1$, $R_x = \infty$, $a/R_y = 0.1$, $E_1/E_2 = 15$)

h/a	Mode	Mode number					
		FCCC	FFCC	FFFC	CFFF	CCFF	CCCF
0.01	1	21.441	5.3519	1.2520	4.7214	5.3519	25.358
	2	23.308	11.164	3.1822	5.1009	11.164	28.704
	3	33.542	23.718	7.8374	10.943	23.718	36.292
	4	38.015	25.838	11.515	23.927	25.838	53.380
0.05	1	10.038	4.4519	1.2491	3.8493	4.4519	21.643
	2	22.125	9.8673	3.1181	4.8754	9.8673	23.978
	3	24.983	22.408	7.7257	10.495	22.408	32.230
	4	33.952	22.695	11.156	21.836	22.695	48.200
0.10	1	8.8956	4.2056	1.2411	3.6585	4.2056	16.423
	2	19.795	9.2023	3.0083	4.5636	9.2023	18.571
	3	20.306	18.167	7.4109	9.8304	18.167	26.348
	4	28.154	20.440	10.139	10.921	20.440	34.952
0.15	1	8.0767	3.9166	1.2282	3.4237	3.9166	12.584
	2	16.565	8.4317	2.8750	4.1729	8.4317	14.695
	3	17.212	14.606	6.9028	7.2807	14.606	21.834
	4	23.254	17.471	6.9649	9.0797	17.471	25.490

cylindrical shell with curved edge cantilevered (CFFF) are higher than those of straight edge cantilevered (FFFC).

Influence of the fiber orientations on the modal frequencies of shallow shells is also investigated. In Fig. 8.5, variations of the lowest three frequency parameters Ω of certain single-layered ([ϑ]) shallow shells with various fiber orientations are given. Three types of curvature considered in the study are: cylindrical ($R_x = \infty$, $a/R_y = 0.1$), spherical ($a/R_x = a/R_y = 0.1$) and hyperbolic paraboloidal ($a/R_x = 0.1$, $a/R_y = -0.1$). In each case, the fiber orientation ϑ is varies from 0° to 180° by an increment of 10°. The shallow shells under consideration are assumed to be with SDSDSDSD boundary conditions. The material constants and geometry parameters of the laminas of the shallow shells are: $b/a = 1$, $h/a = 0.05$, $E_1/E_2 = 15$. Many interesting characteristics can be observed from the figure. The first observation is that all the subfigures are symmetrical about central line (i.e., $\vartheta = 90°$). The second observation is that the fundamental frequency parameter traces climb up and then decline, and may reach their crests around $\vartheta = 45°$ (when ϑ is increased from 0° to 90°). The similar characteristics can be observed in the subfigure of the second mode. However, for the third mode, the maximum frequency parameters may occur around $\vartheta = 30°$ or $\vartheta = 60°$. In addition, it is obvious that frequency parameters of the shallow spherical shell are larger than the shallow cylindrical and hyperbolic paraboloidal ones. Furthermore, since the length-to-radius ratio used in each case in this investigation is small ($a/R = 0.1$), thus, the differences between these results are

Table 8.6 Frequency parameters Ω for a three-layered, [0°/90°/0°] shallow spherical shell with different boundary conditions and thickness-length ratios ($a/b = 1$, $a/R_x = a/R_y = 0.1$, $E_1/E_2 = 15$)

h/a	Mode	Mode number					
		FCCC	FFCC	FFFC	CFFF	CCFF	CCCF
0.01	1	22.125	6.6469	2.4195	4.4589	6.6469	36.435
	2	25.223	12.090	3.2764	5.0746	12.090	39.743
	3	35.576	25.341	10.435	13.354	25.341	45.528
	4	42.189	26.814	11.922	25.096	26.814	60.365
0.05	1	10.101	4.5350	1.3341	3.8447	4.5350	22.313
	2	22.225	9.9327	3.1223	4.8711	9.9327	24.631
	3	25.075	22.393	7.8779	10.657	22.393	32.715
	4	34.138	22.832	11.170	21.583	22.832	48.537
0.10	1	8.9124	4.2279	1.2627	3.6560	4.2279	16.657
	2	19.821	9.2191	3.0095	4.5592	9.2191	18.790
	3	20.325	18.145	7.4477	9.8768	18.145	26.497
	4	28.208	20.485	10.123	10.912	20.485	34.936
0.15	1	8.0840	3.9271	1.2375	3.4215	3.9271	12.723
	2	16.570	8.4387	2.8757	4.1680	8.4387	14.818
	3	17.223	14.587	6.9003	7.2788	14.587	21.912
	4	23.280	17.503	6.9802	9.1028	17.503	25.477

small as well. The maximum differences between the results of cylindrical and spherical shallow shells, cylindrical and hyperbolic paraboloidal shallow shells, spherical and hyperbolic paraboloidal shallow shells are less than 1.14, 0.61, 6.24 %, respectively.

Figure 8.6 performs the similar study for the shallow shells with CCCC boundary conditions. The different observation is that the variation tendencies of the fundamental modes decline firstly and then climb up. The minimum frequency parameters may occur around $\vartheta = 45°$. For the second mode, the frequency parameters increase when ϑ increases from 0° to 40° and decrease when ϑ increases from 50° to 90°. The variation tendencies of the third mode are the same as those in Fig. 8.5. The figure also shows that the differences between the three results are small due to the fact that a low length-to-radius ratio is used in this investigation.

Figure 8.7 shows the similar study for the shallow shells with SDSDSDSD boundary conditions and a higher length-to-radius ratio, i.e., $a/R = 0.2$ (limit of the shallow theory). The material and other geometry properties are the same as those used in Figs. 8.6 and 8.7. The observations from this figure are the same as those of Fig. 8.5. However, the maximum differences between the results of cylindrical and spherical shallow shells, cylindrical and hyperbolic paraboloidal shallow shells, spherical and hyperbolic paraboloidal shallow shells can be as many as 5.29, 6.50, 22.9 %, respectively. It is attributed to the effects of curvatures on the frequency parameters of shallow shells are more significant when the length-to-radius ratio is

Table 8.7 Frequency parameters Ω for a three-layered, [0°/90°/0°] shallow hyperbolic paraboloidal shell with different boundary conditions and thickness-length ratios (a/b = 1, a/R_x = 0.1, a/R_y = −0.1, E_1/E_2 = 15)

h/a	Mode	Mode number					
		FCCC	FFCC	FFFC	CFFF	CCFF	CCCF
0.01	1	22.736	4.935666	2.4375	4.3788	4.9357	36.722
	2	26.242	14.70847	3.2710	5.0823	14.708	38.502
	3	34.129	26.91862	10.876	15.157	26.919	44.979
	4	39.603	27.18928	11.896	25.575	27.189	59.766
0.05	1	10.143	4.429413	1.3368	3.8471	4.4294	22.327
	2	22.268	10.09015	3.1212	4.8706	10.090	24.564
	3	25.002	22.46707	7.8884	10.750	22.467	32.691
	4	34.013	22.82693	11.175	21.644	22.827	48.511
0.10	1	8.9240	4.19818	1.2634	3.6569	4.1982	16.662
	2	19.834	9.264119	3.0085	4.5580	9.2641	18.769
	3	20.302	18.163	7.4502	9.9013	18.163	26.492
	4	28.166	20.48119	10.159	10.917	20.481	34.944
0.15	1	8.0894	3.912118	1.2379	3.4220	3.9121	12.726
	2	16.558	8.461952	2.8748	4.1665	8.4620	14.807
	3	17.230	14.59844	6.9054	7.2823	14.598	21.911
	4	23.255	17.46116	6.9813	9.1142	17.461	25.483

higher. The figure also shows that the variation tendency of each frequency parameter of the cylindrical shallow shell is the same as the corresponding ones of the spherical and hyperbolic paraboloidal shells. Comparing Figs. 8.5, 8.6 and 8.7, it can be found that the influence of fiber orientations on the modal frequencies of shallow shells vary with mode sequence and boundary conditions.

Effects of the fiber orientations on the frequency parameters and mode shapes of laminated shallow shells are further reported. In Tables 8.8, 8.9 and 8.10, the lowest four frequency parameters Ω of certain three-layered, [0°/ϑ/0°] shallow shells with various boundary conditions and fiber orientations are presented. The aspect ratio is chosen to be b/a = 1. The thickness-to-width ratio h/b = 0.1 is used in the calculation. As usual, the shallow cylindrical ($R_x = \infty$, a/R_y = 0.1), spherical ($a/R_x = a/R_y$ = 0.1) and hyperbolic paraboloidal (a/R_x = 0.1, a/R_y = −0.1) shells are considered in the study. The fiber direction angle ϑ is varied from 0° to 90° with an increment of 30°. The layers of the shells are made of composite materials with orthotropy ratio E_1/E_2 = 15. From Table 8.8, it can be noticed that the results of the shell with FFCC boundary conditions equal to those of CCFF boundary conditions. The similar observation can be seen from Tables 8.9 and 8.10 as well.

Figures 8.8, 8.9 and 8.10 give the first three contour plots of the mode shapes and frequency parameters with various lamination angles for CFFF, single-layered [ϑ] shallow cylindrical, spherical and hyperbolic paraboloidal shells, respectively. The aspect ratio a/b = 1, thickness-to-length ratio h/a = 0.05 and orthotropy ratio

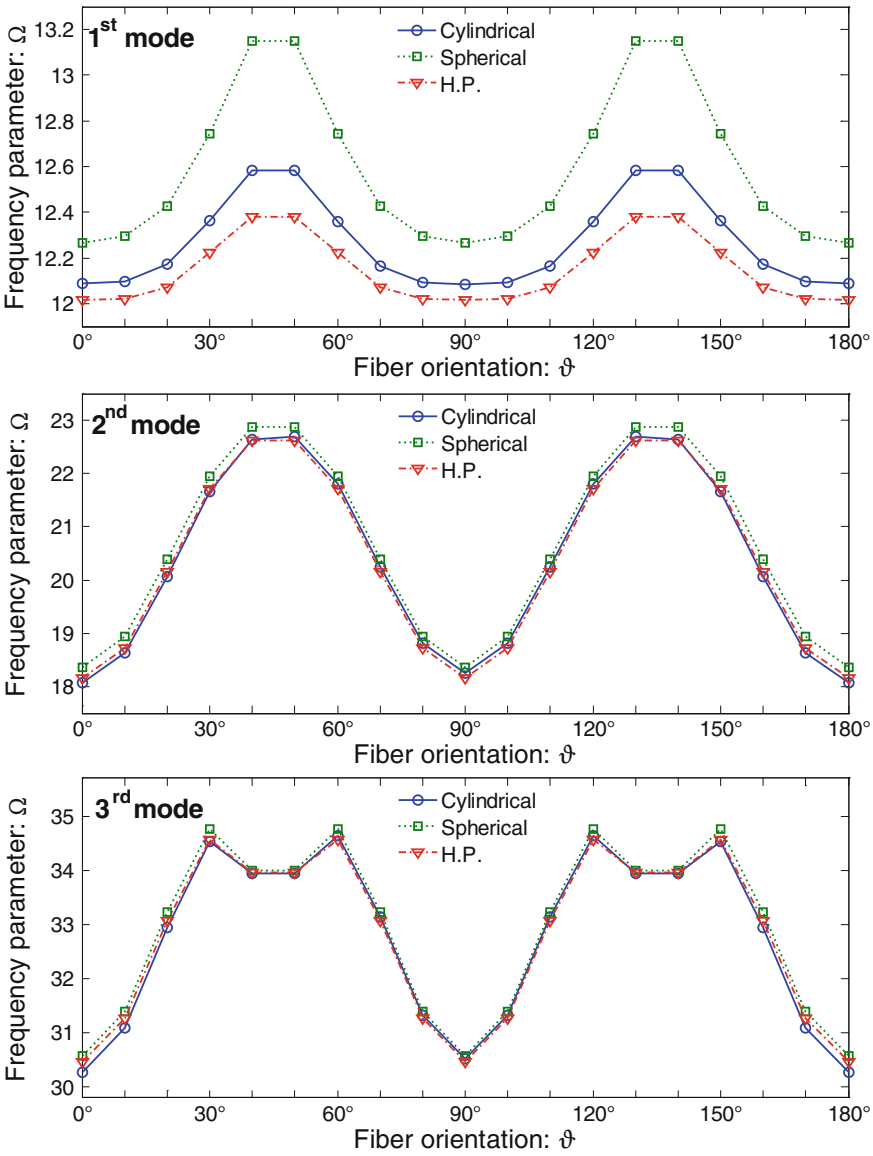

Fig. 8.5 The lowest three frequency parameters Ω of single-layered ([ϑ]) shallow shells with SDSDSDSD boundary condition and various fiber orientations (b/a = 1, h/a = 0.05, a/R = 0.1)

E_1/E_2 = 25 are used in the presentation. Mode shapes and frequency parameters are shown for ϑ = 0, 30°, 60° and 90°. From the figures, we can find that when ϑ = 0, the mode shapes of the shallow cylindrical, spherical and hyperbolic paraboloidal shells

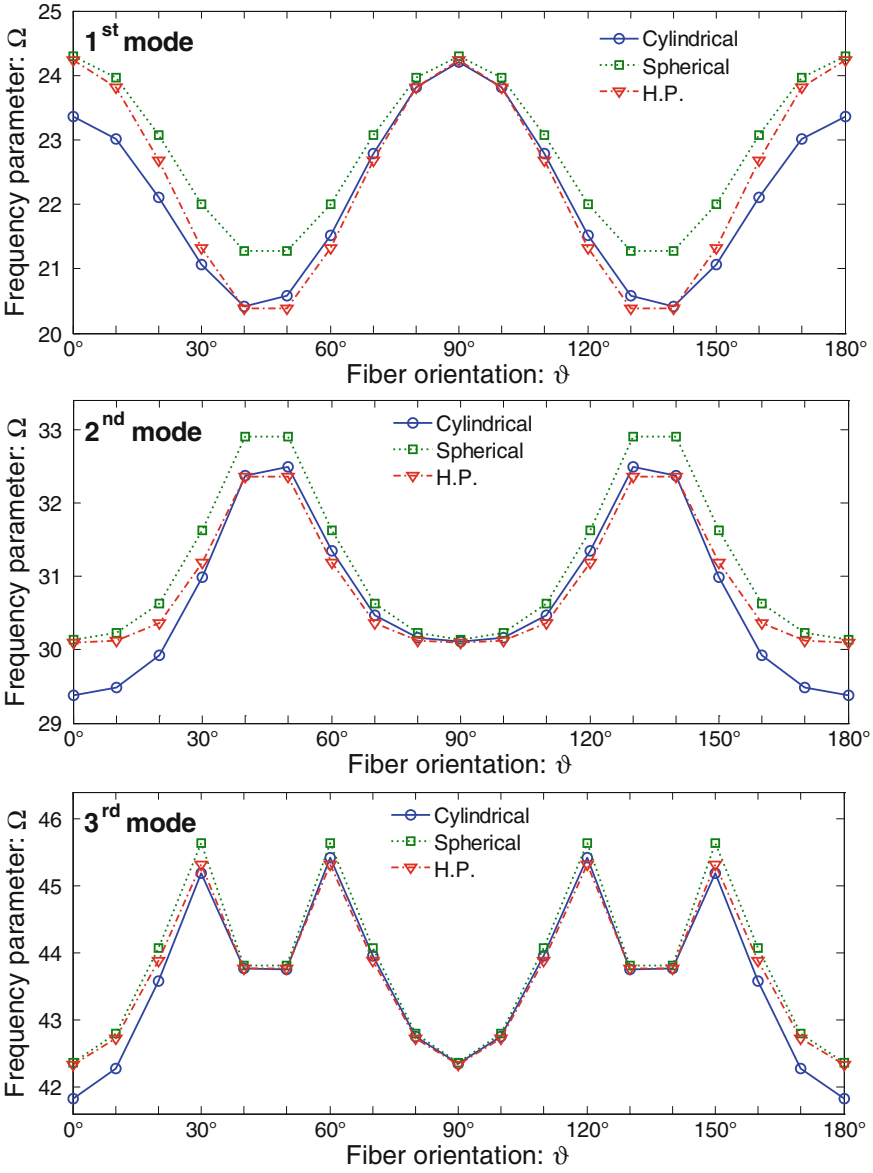

Fig. 8.6 The lowest three frequency parameters Ω of single-layered ([ϑ]) shallow shells with CCCC boundary condition and different fiber orientations (b/a = 1, h/a = 0.05, a/R = 0.1)

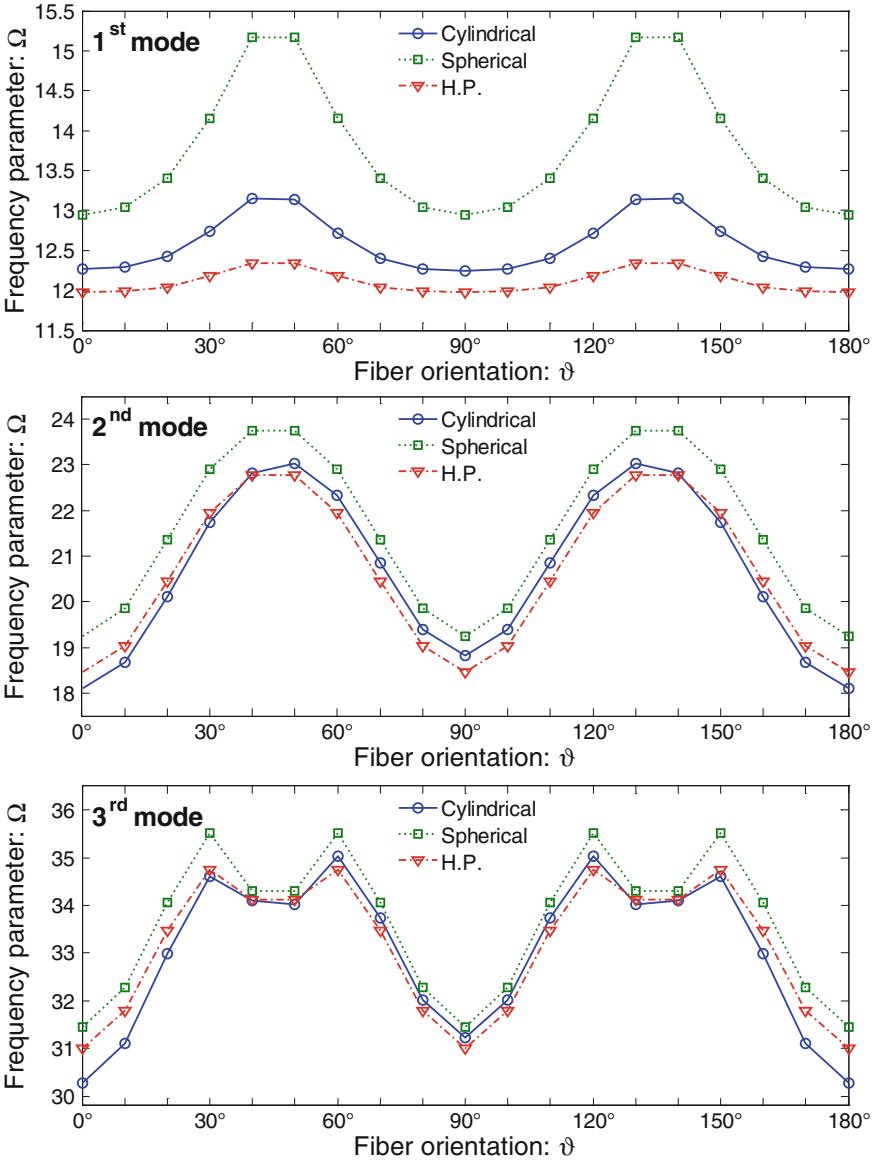

Fig. 8.7 The lowest three frequency parameters Ω of single-layered ([ϑ]) shallow shells with SDSDSDSD boundary condition and different fiber orientations (b/a = 1, h/a = 0.05, a/R = 0.2)

Table 8.8 Frequency parameters Ω for a three-layered, [0°/ϑ/0°] shallow cylindrical shell with different boundary conditions and fiber orientations (a/b = 1, h/a = 0.1, $R_x = \infty$, a/R_y = 0.1, E_1/E_2 = 15)

ϑ	Mode	Boundary conditions						
		FFFC	FFCC	FCCC	CCCC	CCCF	CCFF	CFFF
0°	1	1.0086	4.1935	7.6932	18.084	16.790	4.1935	3.7272
	2	2.8658	8.2303	16.985	23.818	18.445	8.2303	4.6176
	3	6.0857	17.494	20.188	34.495	24.372	17.494	8.8185
	4	7.1446	18.539	26.655	36.670	28.413	18.539	11.145
30°	1	1.0255	4.2544	7.8266	18.081	16.690	4.2544	3.6999
	2	3.0243	8.4954	17.287	24.067	18.506	8.4954	4.6980
	3	6.1868	17.845	20.260	34.990	24.685	17.845	9.0384
	4	8.2781	18.522	27.064	36.540	35.586	18.522	14.682
60°	1	1.1380	4.2553	8.4006	18.180	16.509	4.2553	3.6655
	2	3.0852	9.0720	18.670	24.977	18.569	9.0720	4.6604
	3	6.8488	18.270	20.334	36.237	25.658	18.270	9.5119
	4	9.8179	19.325	27.760	37.001	35.157	19.325	13.338
90°	1	1.2411	4.2056	8.8956	18.288	16.423	4.2056	3.6585
	2	3.0083	9.2023	19.795	25.634	18.571	9.2023	4.5636
	3	7.4109	18.167	20.306	36.071	26.348	18.167	9.8304
	4	10.139	20.440	28.154	38.556	34.952	20.440	10.921

Table 8.9 Frequency parameters Ω for a three-layered, [0°/ϑ/0°] shallow spherical shell with different boundary conditions and fiber orientations (a/b = 1, h/a = 0.1, $a/R_x = a/R_y$ = 0.1, E_1/E_2 = 15)

ϑ	Mode	Boundary conditions						
		FFFC	FFCC	FCCC	CCCC	CCCF	CCFF	CFFF
0°	1	1.0154	4.2034	7.7061	18.405	17.124	4.2034	3.7246
	2	2.8665	8.2380	17.010	24.060	18.756	8.2380	4.6131
	3	6.1081	17.534	20.201	34.662	24.601	17.534	8.8466
	4	7.1418	18.517	26.706	36.665	28.418	18.517	11.135
30°	1	1.0337	4.2659	7.8541	18.388	16.976	4.2659	3.6970
	2	3.0252	8.5066	17.329	24.284	18.783	8.5066	4.6937
	3	6.2174	17.892	20.297	35.138	24.887	17.892	9.0737
	4	8.2752	18.510	27.144	36.544	35.579	18.510	14.641
60°	1	1.1525	4.2700	8.4395	18.439	16.748	4.2700	3.6627
	2	3.0868	9.0865	18.706	25.148	18.803	9.0865	4.6564
	3	6.8821	18.248	20.374	36.246	25.821	18.248	9.5526
	4	9.8140	19.381	27.828	37.117	35.147	19.381	13.313
90°	1	1.2627	4.2279	8.9124	18.510	16.657	4.2279	3.6560
	2	3.0095	9.2191	19.821	25.791	18.790	9.2191	4.5592
	3	7.4477	18.145	20.325	36.068	26.497	18.145	9.8768
	4	10.123	20.485	28.208	38.661	34.936	20.485	10.912

Table 8.10 Frequency parameters Ω for a three-layered, [0°/ϑ/0°] shallow hyperbolic paraboloidal shell with different boundary conditions and fiber orientations ($a/b = 1$, $h/a = 0.1$, $a/R_x = 0.1$, $a/R_y = -0.1$, $E_1/E_2 = 15$)

ϑ	Mode	Boundary conditions						
		FFFC	FFCC	FCCC	CCCC	CCCF	CCFF	CFFF
0°	1	1.0157	4.1873	7.7187	18.386	17.124	4.1873	3.7256
	2	2.8653	8.2775	17.026	24.050	18.738	8.2775	4.6122
	3	6.1094	17.538	20.183	34.655	24.596	17.538	8.8732
	4	7.1476	18.505	26.670	36.658	28.411	18.505	11.140
30°	1	1.0341	4.2485	7.8638	18.312	16.953	4.2485	3.6985
	2	3.0238	8.5641	17.344	24.249	18.735	8.5641	4.6926
	3	6.2200	17.904	20.263	35.119	24.861	17.904	9.1066
	4	8.2838	18.501	27.099	36.529	35.567	18.501	14.653
60°	1	1.1531	4.2492	8.4234	18.363	16.743	4.2492	3.6641
	2	3.0852	9.1477	18.718	25.127	18.763	9.1477	4.6551
	3	6.8868	18.258	20.324	36.219	25.805	18.258	9.5801
	4	9.8311	19.378	27.781	37.102	35.140	19.378	13.324
90°	1	1.2634	4.1982	8.9240	18.492	16.662	4.1982	3.6569
	2	3.0085	9.2641	19.834	25.782	18.769	9.2641	4.5580
	3	7.4502	18.163	20.302	36.060	26.492	18.163	9.9013
	4	10.159	20.481	28.166	38.655	34.944	20.481	10.917

are symmetrical with respect to the longitudinal center line. It is attributed to the boundary conditions, geometry and material properties of the shallow shells under consideration are symmetrical with respect to the longitudinal center line as well. Furthermore, it is obviously that the maximum frequency parameters for the first, second and third modes in each case occur at $\vartheta = 0$, $\vartheta = 0$ and $\vartheta = 30°$, respectively. The figures also show that that the node lines (i.e., lines with zero displacements) of the mode shapes vary with respect to the fiber orientation. In addition, since the length-to-radius ratio used in this investigation is small ($a/R = 0.1$), thus, the differences between the frequency parameters are small as well.

Tables 8.11, 8.12 and 8.13 present the first four non-dimension frequency parameters Ω of certain two-layered, angle-ply [45°/−45°] shallow cylindrical, spherical and hyperbolic paraboloidal shells with different boundary conditions and length-to-radius ratios, respectively. Four different length-to-radius ratios i.e. $a/R = 0.05$, 0.1, 0.15 and 0.2, corresponding to considerably to slightly shallow shells are performed in the analysis. The shells are formed in rectangular planform with following geometry and material properties: $a/b = 1/2$, $h/a = 0.1$, $E_1/E_2 = 15$, $R_x = \infty$ for shallow cylindrical shells, $R_y = R_x$ for the spherical shells and $R_y = -R_x$ for the hyperbolic paraboloidal ones. Seven different boundary conditions, i.e.,

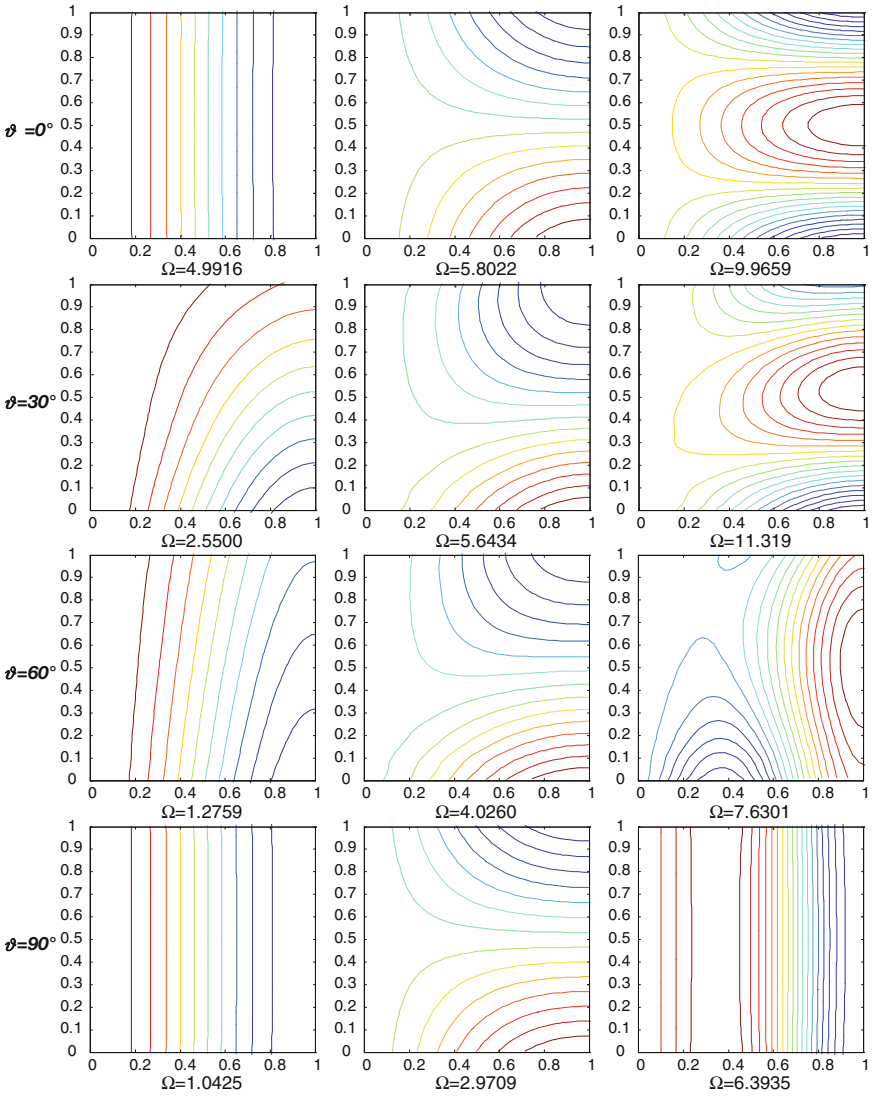

Fig. 8.8 Mode shapes and frequency parameters for CFFF shallow cylindrical shells ([9], $a/b = 1$, $h/a = 0.05$, $R_x = \infty$, $a/R_y = 0.1$, $E_1/E_2 = 25$)

FFFC, FFCC, FCCC, CCCC, CCCF, CCFF and CFFF are performed in the calculation. It can be seen from the table that the augmentation of the length-to-radius ratio leads to the increases of the frequency parameters. Table 8.11 also shows that the results of shallow cylindrical shells cantilevered in the curved edge (CFFF) are

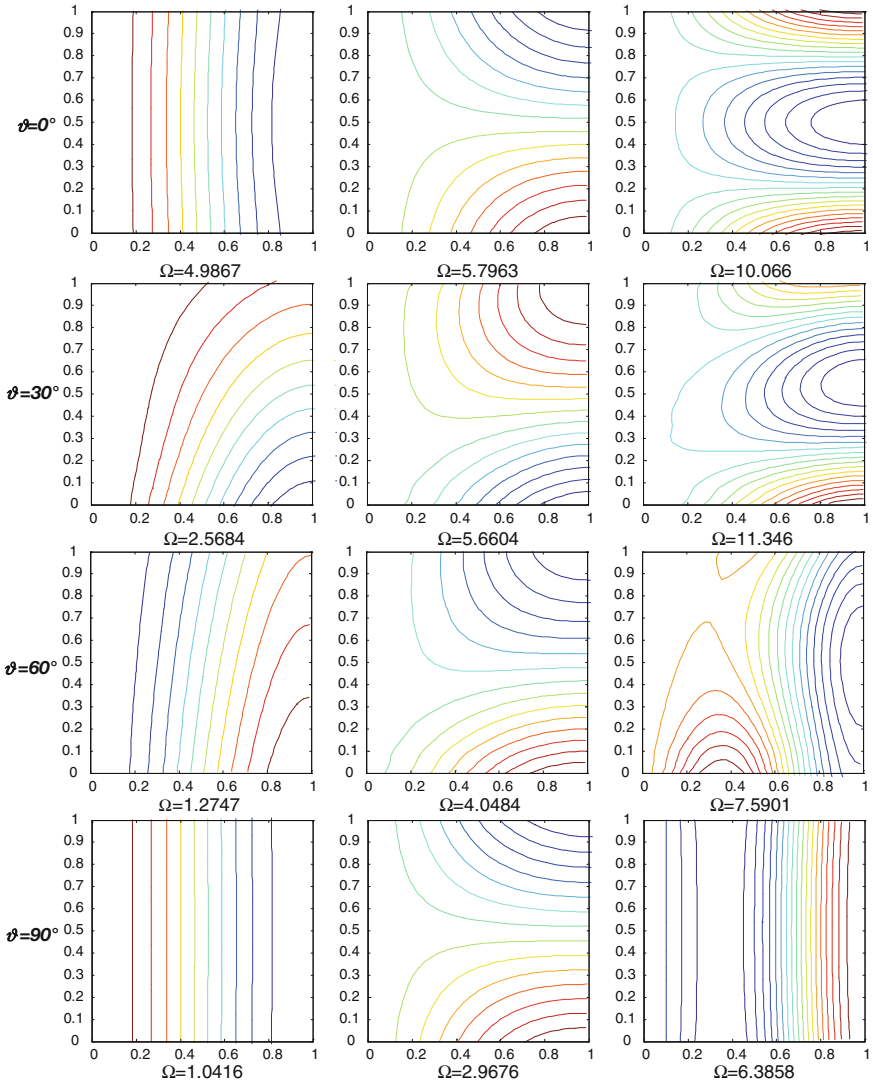

Fig. 8.9 Mode shapes and frequency parameters for CFFF shallow spherical shells ([9], $a/b = 1$, $h/a = 0.05$, $a/R_x = a/R_y = 0.1$, $E_1/E_2 = 25$)

higher than those of straight edge cantilevered (FFFC). From Table 8.12, it can be noticed that the results for the spherical shells with FFCC boundary conditions equal to those of CCFF boundary conditions. The similar observation can be seen from Tables 8.10 and 8.13 as well.

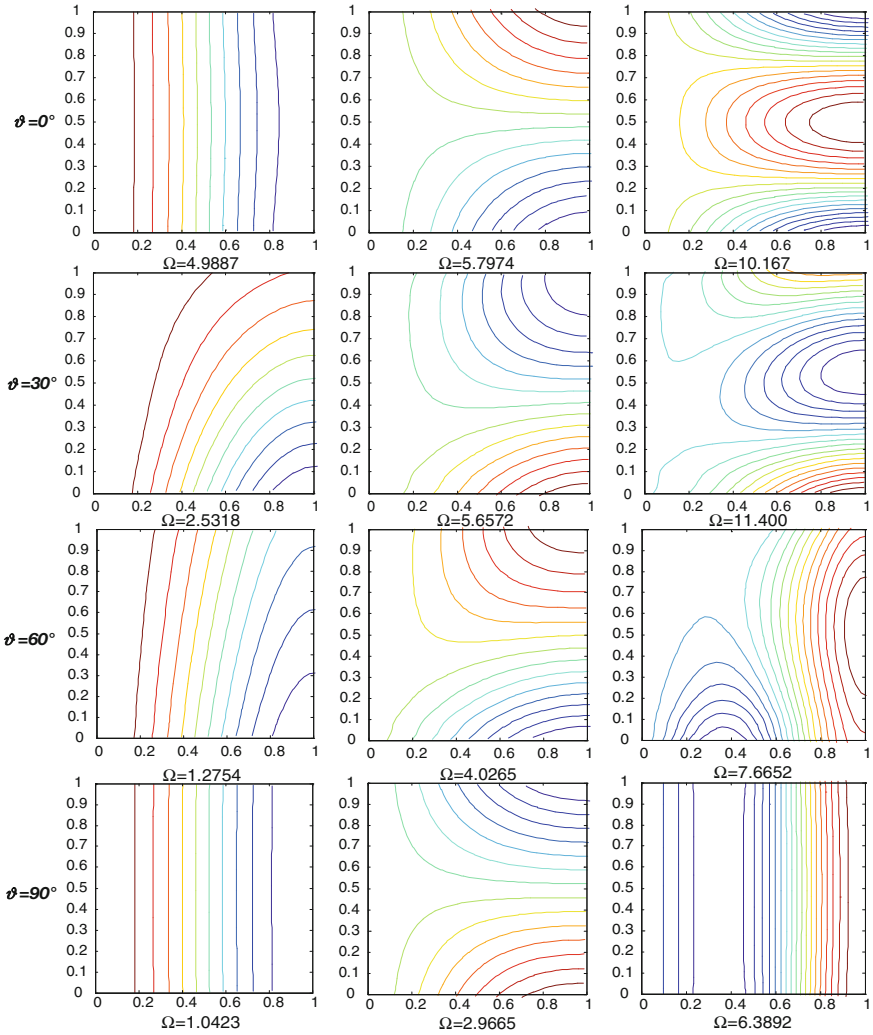

Fig. 8.10 Mode shapes and frequency parameters for CFFF hyperbolic paraboloidal shallow shells ([9], $a/b = 1$, $h/a = 0.05$, $a/R_x = 0.1$, $a/R_y = -0.1$, $E_1/E_2 = 25$)

As the last case, parameter studies are carried out in Figs. 8.11 and 8.12 to further investigate the effects of length-to-radius ratios a/R_x and a/R_y on the frequency parameters Ω of laminated shallow shells. Figure 8.11 depicts the lowest three frequency parameters Ω versus length-to-radius ratios a/R_x and a/R_y for a [0°/90°] layered shallow shell with aspect ratio of $a/b = 5$ and CCCC boundary conditions. The other shell parameters used in the study are: $h/b = 0.1$, $E_1/E_2 = 15$. It is

Table 8.11 Frequency parameters Ω for two-layered, angle-ply [45°/−45°] shallow cylindrical shells with different boundary conditions and length-to-radius ratios (a/b = 1/2, h/a = 0.1, $R_x = \infty$, E_1/E_2 = 15)

a/R_y	Mode	Boundary conditions						
		FFFC	FFCC	FCCC	CCCC	CCCF	CCFF	CFFF
0.05	1	0.3640	2.0340	3.6812	10.195	9.1129	2.0340	1.5413
	2	2.0500	4.4388	7.6647	13.482	11.007	4.4388	2.7424
	3	2.2144	8.1038	11.116	18.452	14.501	8.1038	5.0423
	4	3.5598	9.4052	13.149	23.372	19.455	9.4052	8.5097
0.10	1	0.3636	2.1008	3.8405	10.323	9.1883	2.1008	1.6328
	2	2.0169	4.4927	7.6996	13.551	11.083	4.4927	2.7494
	3	2.2112	8.1231	11.192	18.484	14.542	8.1231	5.0531
	4	3.5724	9.4414	13.162	23.406	19.473	9.4414	8.5117
0.15	1	0.3629	2.2068	4.0909	10.532	9.3066	2.2068	1.7725
	2	1.9665	4.5838	7.7572	13.666	11.212	4.5838	2.7610
	3	2.2049	8.1551	11.317	18.536	14.611	8.1551	5.0715
	4	3.5903	9.5079	13.185	23.463	19.503	9.5079	8.5150
0.20	1	0.3620	2.3364	4.4152	10.819	9.4581	2.3364	1.9466
	2	1.9036	4.7125	7.8367	13.825	11.398	4.7125	2.7771
	3	2.1953	8.1996	11.488	18.609	14.708	8.1996	5.0981
	4	3.6104	9.6029	13.218	23.542	19.545	9.6029	8.5196

Table 8.12 Frequency parameters Ω for two-layered, angle-ply [45°/−45°] shallow spherical shells with different boundary conditions and length-to-radius ratios (a/b = 1/2, h/a = 0.1, $R_y = R_x$, E_1/E_2 = 15)

a/R_y	Mode	Boundary conditions						
		FFFC	FFCC	FCCC	CCCC	CCCF	CCFF	CFFF
0.05	1	0.3645	2.0354	3.6866	10.290	9.1764	2.0354	1.5399
	2	2.0508	4.4309	7.6754	13.543	11.072	4.4309	2.7416
	3	2.2162	8.1005	11.130	18.488	14.546	8.1005	5.0389
	4	3.5581	9.4006	13.161	23.374	19.483	9.4006	8.5105
0.10	1	0.3655	2.1093	3.8597	10.694	9.4250	2.1093	1.6277
	2	2.0196	4.4727	7.7416	13.793	11.347	4.4727	2.7464
	3	2.2188	8.1290	11.246	18.626	14.720	8.1290	5.0392
	4	3.5660	9.4297	13.211	23.415	19.582	9.4297	8.5143
0.15	1	0.3671	2.2279	4.1272	11.334	9.7832	2.2279	1.7618
	2	1.9718	4.5443	7.8480	14.198	11.816	4.5443	2.7543
	3	2.2222	8.1815	11.432	18.854	15.009	8.1815	5.0396
	4	3.5769	9.4847	13.295	23.483	19.747	9.4847	8.5199
0.20	1	0.3692	2.3752	4.4659	12.168	10.196	2.3752	1.9296
	2	1.9115	4.6421	7.9895	14.744	12.482	4.6421	2.7652
	3	2.2259	8.2561	11.680	19.168	15.409	8.2561	5.0396
	4	3.5886	9.5615	13.415	23.578	19.976	9.5615	8.5260

Table 8.13 Frequency parameters Ω for two-layered, angle-ply [45°/−45°] shallow hyperbolic paraboloidal shells with different boundary conditions and length-to-radius ratios (a/b = 1/2, h/a = 0.1, $R_y = -R_x$, E_1/E_2 = 15)

a/R_x	Mode	Boundary conditions						
		FFFC	FFCC	FCCC	CCCC	CCCF	CCFF	CFFF
0.05	1	0.3650	2.0546	3.6876	10.178	9.1143	2.0546	1.5421
	2	2.0492	4.4454	7.6736	13.476	11.005	4.4454	2.7422
	3	2.2213	8.1058	11.111	18.454	14.503	8.1058	5.0559
	4	3.5615	9.4232	13.155	23.370	19.460	9.4232	8.5239
0.10	1	0.3677	2.1351	3.8650	10.258	9.1955	2.1351	1.6340
	2	2.0144	4.5292	7.7353	13.531	11.070	4.5292	2.7488
	3	2.2381	8.1494	11.170	18.491	14.548	8.1494	5.1079
	4	3.5788	9.4751	13.189	23.400	19.492	9.4751	8.5679
0.15	1	0.3718	2.2438	4.1437	10.389	9.3293	2.2438	1.7680
	2	1.9620	4.6741	7.8368	13.621	11.179	4.6741	2.7593
	3	2.2633	8.2275	11.269	18.551	14.624	8.2275	5.1953
	4	3.6036	9.5554	13.245	23.450	19.546	9.5554	8.6406
0.20	1	0.3773	2.3628	4.5045	10.571	9.5130	2.3628	1.9247
	2	1.8974	4.8796	7.9764	13.746	11.330	4.8796	2.7734
	3	2.2949	8.3391	11.405	18.636	14.730	8.3391	5.3187
	4	3.6320	9.6628	13.324	23.520	19.621	9.6628	8.7404

seen that each frequency parameter Ω of the shell increases with the increments of length-to-radius ratios a/R_x or a/R_y. The figure also shows that the effects of length-to-radius ratios a/R_x and a/R_y on the frequency parameters Ω of laminated shallow shells vary with mode sequence.

Figure 8.12 shows the similar study for the shallow shell with aspect ratio of a/b = 1. The figure shows that the fundamental frequency parameter Ω of the shell increases with the increase of length-to-radius ratios a/R_x or a/R_y. However, for the second mode, the maximum and minimum frequency parameters occur at a/R_x = 0.2, $a/R_y = -0.2$ and a/R_x = 0, a/R_y = 0.2, respectively. And for the third mode, the minimum and maximum frequency parameters occur at $a/R_x = a/R_y = 0$ (plate) and $a/R_x = a/R_y = 0.2$ (spherical curvature), respectively. Figures 8.11 and 8.12 also reveal that the effects of length-to-radius ratios on the vibration characteristics of shallow shells vary with aspect ratios.

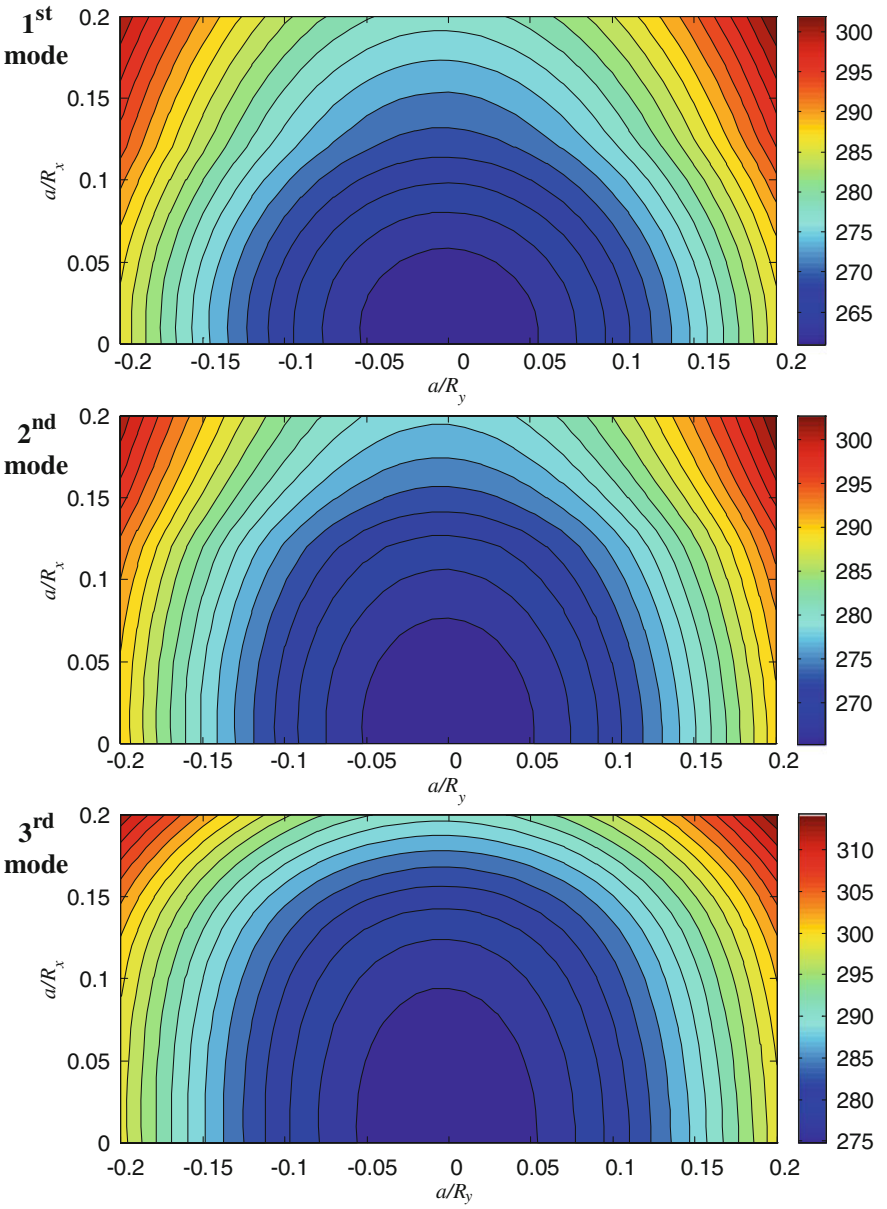

Fig. 8.11 The lowest three frequency parameters Ω versus length-to-radius ratios a/R_x and a/R_y for a [0°/90°] layered shallow shell with aspect ratio of $a/b = 5$

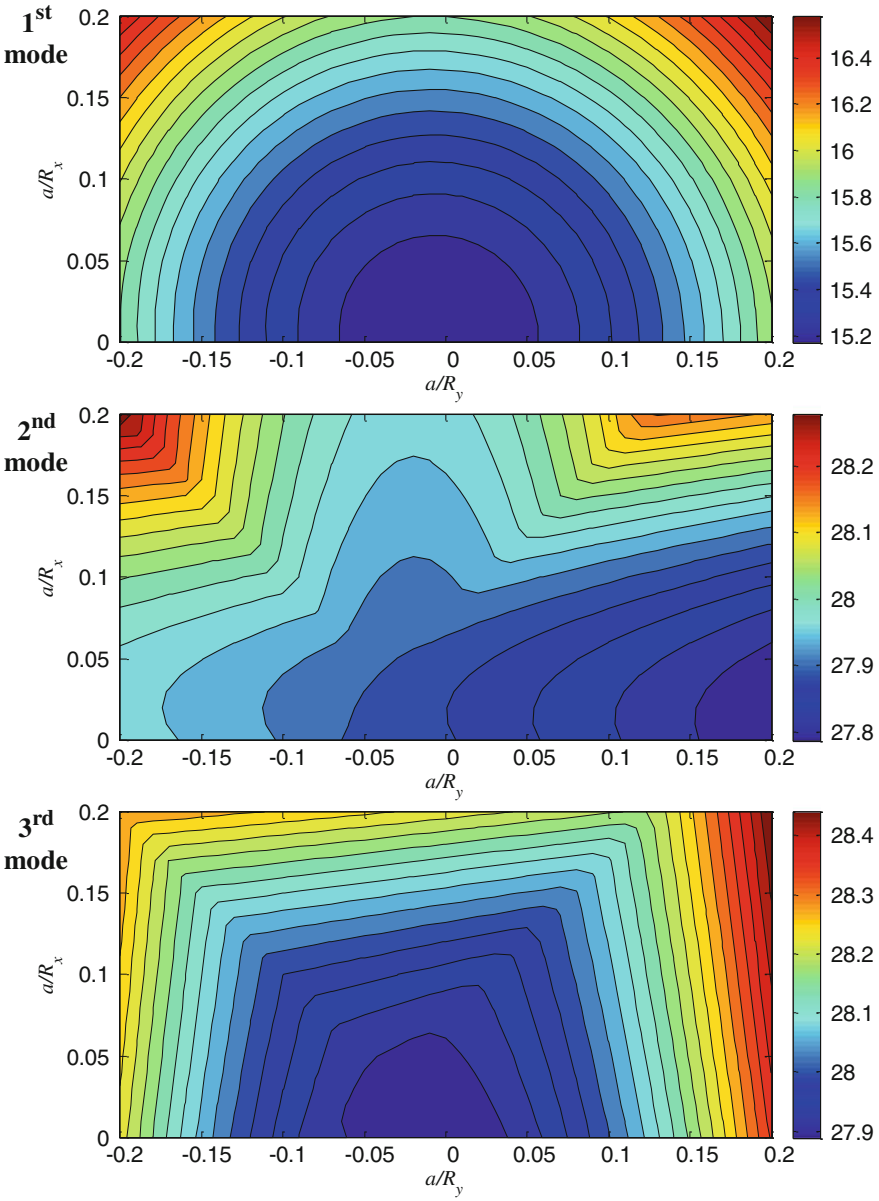

Fig. 8.12 The lowest three frequency parameters Ω versus length-to-radius ratios a/R_x and a/R_y for a [0°/90°] layered shallow shell with aspect ratio of $a/b = 1$